Journal of Vertebrate Paleontology

Taylor & Francis
Taylor & Francis Group

ISSN: 0272-4634 (Print) 1937-2809 (Online) Journal homepage: www.tandfonline.com/journals/ujvp20

Redescription of the *Panoplosaurus mirus* (Ankylosauria: Nodosauridae) holotype skull using computed tomography, and a new comparative scheme for panoplosaurin cranial ornamentation

Marissa C. H. Livius, Lawrence M. Witmer, Michael J. Ryan, Hillary C. Maddin & Jordan C. Mallon

To cite this article: Marissa C. H. Livius, Lawrence M. Witmer, Michael J. Ryan, Hillary C. Maddin & Jordan C. Mallon (07 Apr 2026): Redescription of the *Panoplosaurus mirus* (Ankylosauria: Nodosauridae) holotype skull using computed tomography, and a new comparative scheme for panoplosaurin cranial ornamentation, Journal of Vertebrate Paleontology, DOI: 10.1080/02724634.2026.2636589

To link to this article: https://doi.org/10.1080/02724634.2026.2636589

© 2026 Marissa C.H. Livius, Lawrence M. Witmer, Michael J. Ryan, Hillary C. Maddin and Jordan C. Mallon

Published online: 07 Apr 2026.

Submit your article to this journal

View related articles

View Crossmark data

Full Terms & Conditions of access and use can be found at
https://www.tandfonline.com/action/journalInformation?journalCode=ujvp20

Journal of Vertebrate Paleontology e2636589 (27 pages)
Published with license by the Society of Vertebrate Paleontology.
DOI: 10.1080/02724634.2026.2636589

Check for updates

ARTICLE

REDESCRIPTION OF THE *PANOPLOSAURUS MIRUS* (ANKYLOSAURIA: NODOSAURIDAE) HOLOTYPE SKULL USING COMPUTED TOMOGRAPHY, AND A NEW COMPARATIVE SCHEME FOR PANOPLOSAURIN CRANIAL ORNAMENTATION

MARISSA C. H. LIVIUS, [1*] LAWRENCE M. WITMER, [2] MICHAEL J. RYAN, [1,3] HILLARY C. MADDIN, [1] and JORDAN C. MALLON [1,3]

[1]Ottawa-Carleton Geoscience Centre and Department of Earth Sciences, Carleton University, Ottawa, Ontario K1S 5B6, Canada, marissalivius@gmail.com; michaelpjryan@gmail.com; hillarymaddin@cunet.carleton.ca;

[2]Department of Biomedical Sciences, Heritage College of Osteopathic Medicine, Ohio Center for Ecology and Evolutionary Studies, Ohio University, Athens, Ohio 45701, U.S.A., witmerL@ohio.edu;

[3]Beaty Centre for Species Discovery and Palaeobiology Section, Canadian Museum of Nature, Ottawa, Ontario K1P 6P4, Canada, jmallon@nature.ca

ABSTRACT—The late Campanian nodosaurid *Panoplosaurus mirus* Lambe 1919 was named on the basis of a complete skull and partial postcranium. However, as is typical of ankylosaurs, the constituent elements of the holotype skull (CMN 2759) are obscured both by their extensive co-ossification and by the overlying bony caputegulae, complicating taxonomic referral of other material. The holotype skull is re-examined here using computed tomography (CT) imaging, revealing new information about the internal anatomy. Previously unknown regions of the skull are described, including the basicranium and palate, and the internal anatomy in *Panoplosaurus* is examined from CT-rendered models of the brain and nasal cavities. The occurrence of a vomerine canal or groove and convoluted nasal passages are confirmed in *Panoplosaurus*, while decreased brain flexure relative to other nodosaurids suggests there is greater variability in the paleoneurology of Nodosauridae than previously appreciated. The unique pattern of cranial ornamentation in *Panoplosaurus* is also determined to be taxonomically significant (as it is in Ankylosauridae), and the generic separation of *Panoplosaurus* and the closely related *Edmontonia* is supported. Further, intraspecific variation in the cranial ornamentation of *Panoplosaurus* is revealed, based on the presence or absence of the internasal caputegulum, although the nature of this variation (e.g., ontogeny, sexual dimorphism, individual variation) remains elusive.

Citation for this article: Livius, M. C. H., Witmer, L. M., Ryan, M. J., Maddin, H. C., & Mallon, J. C. (2026) Redescription of the *Panoplosaurus mirus* (Ankylosauria: Nodosauridae) holotype skull using computed tomography, and a new comparative scheme for panoplosaurin cranial ornamentation. *Journal of Vertebrate Paleontology*. https://doi.org/10.1080/02724634.2026.2636589

Submitted: June 25, 2025
Revisions received: December 15, 2025
Accepted: January 29, 2026

INTRODUCTION

Overview of Ankylosauria

Ankylosauria is a clade of herbivorous ornithischian dinosaurs whose earliest known members occur in the Middle Jurassic of Europe, Asia, and Africa, and which achieved a global distribution by the Late Cretaceous (Carpenter, 2004; Dong, 1993; Galton, 1983; Maidment et al., 2021; Vickaryous et al., 2004). Colloquially known as the "armored dinosaurs," ankylosaurs were bulky, low-browsing quadrupeds with dermal ossifications covering extensive portions of the head and body (Vickaryous et al., 2004). The seminal work of Coombs (1978) provided the first systematic organization of a previously chaotic Ankylosauria, with the identification of two main families, Ankylosauridae and Nodosauridae (Vickaryous et al., 2004). While Coombs (1978) found significant morphological differences between ankylosaurids and nodosaurids, he noted a lack of diversity within the families, which has made systematic work at the family level difficult (Thompson et al., 2012). Nodosaurid phylogeny has undergone several revisions since then, but the interrelationships remain poorly understood (Arbour & Currie, 2016; Bakker, 1988; Burns, 2015; Carpenter, 1990; Lee, 1996; Rivera-Sylva et al., 2018; Thompson et al., 2012). Recently, Nodosauridae was recovered as paraphyletic by Raven et al. (2023), and Coombs' (1978) traditional dichotomy was not supported. Instead, four ankylosaur clades, Ankylosauridae, Panoplosauridae, Polacanthidae, and Struthiosauridae, were identified (Raven et al., 2023). However, this result has not yet been independently replicated, and given both the historical entrenchment of Nodosauridae and the recovery of its

*Corresponding author.
© 2026 Marissa C.H. Livius, Lawrence M. Witmer, Michael J. Ryan, Hillary C. Maddin and Jordan C. Mallon. This is an Open Access article distributed under the terms of the Creative Commons Attribution-NonCommercial-NoDerivatives License (http://creativecommons.org/licenses/by-nc-nd/4.0/), which permits non-commercial re-use, distribution, and reproduction in any medium, provided the original work is properly cited, and is not altered, transformed, or built upon in any way. The terms on which this article has been published allow the posting of the Accepted Manuscript in a repository by the author(s) or with their consent.

Color versions of one or more of the figures in the article can be found online at www.tandfonline.com/ujvp.

Published online 07 Apr 2026

monophyly in other recent studies (Arbour & Currie, 2016; Rivera-Sylva et al., 2018; Thompson et al., 2012), we opt to continue to use it here, acknowledging that new data may continue to overturn the consensus.

Taxonomic History of *Panoplosaurus* and *Edmontonia*

The taxonomy of certain nodosaurid specimens has also been problematic, for which the North American nodosaurids *Panoplosaurus* and *Edmontonia* (recovered within Panoplosauridae by Raven et al., 2023) are prime examples (Bakker, 1988; Burns, 2015; Carpenter, 1990; Coombs, 1971, 1978; Gangloff, 1995). Since the holotype skeleton (CMN 2759) of *Pan. mirus* Lambe, 1919 was first described and named from the upper Campanian Dinosaur Park Formation of Alberta (Fig. 1), its validity has never been challenged, and it remains the oldest named taxon still considered valid among North American nodosaurids of the Upper Cretaceous (Coombs & Deméré, 1996; Lambe, 1919). However, the taxonomy of closely related genera, particularly *Edmontonia*, is historically convoluted and unstable (Bakker, 1988; Burns, 2015; Carpenter, 1990; Coombs, 1971). The type species, *Edmontonia longiceps* Sternberg, 1928 (holotype CMN 8531), was named based on material collected from the Horseshoe Canyon Formation in Alberta (uppermost Campanian–Maastrichtian, 73.1–68 Ma; Fig. 1; Eberth & Kamo, 2020). Sternberg (1928) found that the skull resembled that of *Pan. mirus* but considered it generically distinct due to differences in cranial proportions. The validity of *Edmontonia* was first challenged by Gilmore (1930) when he described a nodosaurid (*Edmontonia rugosidens*, holotype USNM 11868) from the Two Medicine Formation in Montana (Campanian, 78.2–74.6 Ma; Fig. 1; Ramezani et al., 2022). He noted a strong resemblance of the skull and caputegulae (cranial ornamentation) to an unnamed species of *Palaeoscincus* (AMNH 5665) discussed in a popular article by Matthew (1922) and erected the new species *Palaeoscincus rugosidens* Gilmore, 1930. Gilmore (1930) also found that the caputegulae and palatal morphology of *Pal. rugosidens* was markedly similar to that of *Ed. longiceps*. Consequently, he doubted there was enough morphological evidence to support the genus *Edmontonia* and suggested that the two species were congeneric (Gilmore, 1930). Russell (1940) agreed that the species were of the same genus but argued against referring additional specimens to *Palaeoscincus* due to the inadequacy of the type material (a single tooth described by Leidy [1856]; *Palaeoscincus* has since been considered a nomen dubium; Vickaryous et al., 2004). Instead, Russell (1940) proposed reassigning Gilmore's (1930) species to *Edmontonia*, as *Ed. rugosidens*. Further, Russell (1940) described a well-preserved nodosaurid (ROM 1215) collected from the Dinosaur Park Formation in Alberta (upper Campanian, 76.4–74.4 Ma; Ramezani et al., 2022) and referred it to *Ed. rugosidens* based on nearly identical cranial anatomy. Consistent with earlier work, Russell (1940) considered *Edmontonia* (= "*Palaeoscincus*") as generically distinct from *Panoplosaurus*, and the recognition of two genera and three species, *Pan. mirus*, *Ed. longiceps*, and *Ed. rugosidens*, went uncontested for another 30 years.

In preparation for his major revision of the Ankylosauria, Coombs (1978) performed a comprehensive examination of the ankylosaur material known at the time, including the specimens

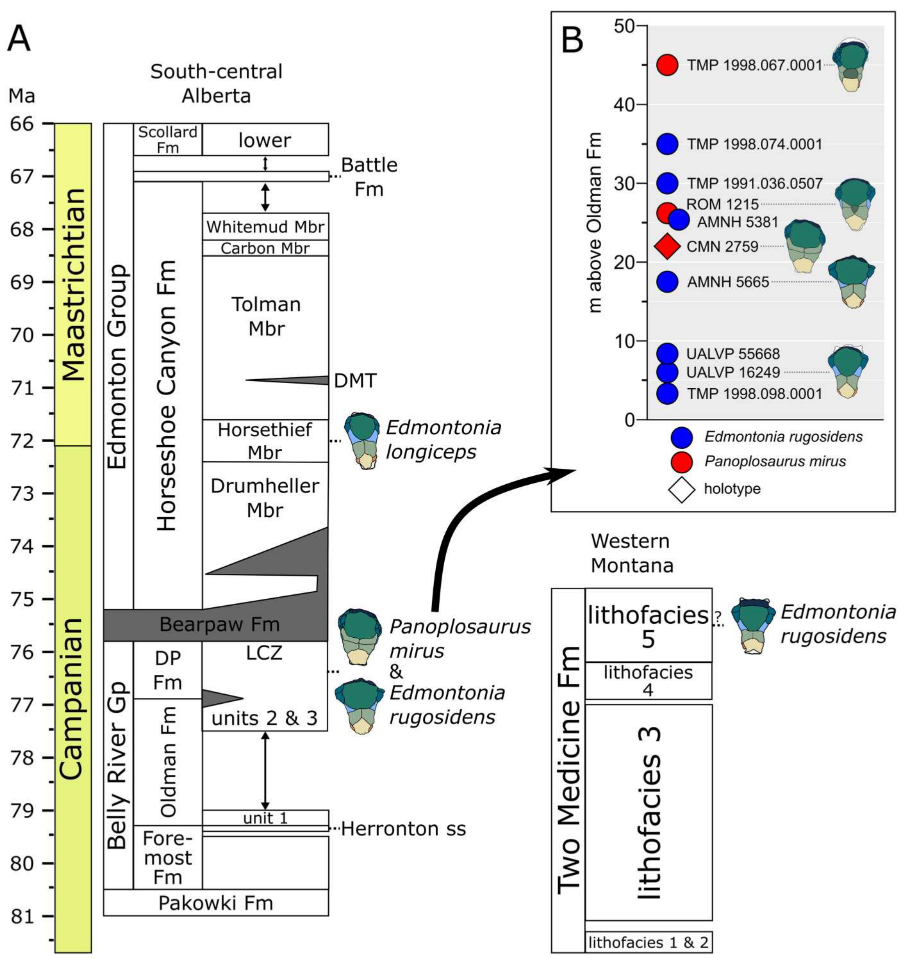

FIGURE 1. Stratigraphic distribution of *Panoplosaurus* and *Edmontonia*. **A**, stratigraphic distribution of *Panoplosaurus mirus* and *Edmontonia* spp. in Upper Cretaceous deposits of Alberta and Montana (single purported occurrence of cf. *Panoplosaurus mirus* in Alaska not shown). Stratigraphic correlations after Fowler (2017); **B**, stratigraphic distribution of *Pan. mirus* and *Edmontonia rugosidens* in the Dinosaur Park Formation of Alberta. **Abbreviations**: **DMT**, Drumheller Marine Tongue; **DP**, Dinosaur Park; **Fm**, Formation; **Gr**, Group; **LCZ**, Lethbridge Coal Zone; **Mbr**, Member.

TABLE 1. Historical taxonomic referrals for specimens of *Panoplosaurus* and *Edmontonia*. Only specimens with conflicting referrals have been included (CMN 2759 excepted). Holotype specimens are denoted by an asterisk.

Specimen	Taxonomic Referrals
AMNH 3076	*Panoplosaurus rugosidens* (Coombs, 1971); *Edmontonia* sp. (Carpenter, 1990); *Edmontonia longiceps* (Burns, 2015; Stanford et al., 2011).
AMNH 5381	*Panoplosaurus rugosidens* (Coombs, 1971); *Edmontonia* (*Chassternbergia*) sp. (Bakker, 1988); *Edmontonia rugosidens* (Burns, 2015; Carpenter, 1990; Stanford et al., 2011).
AMNH 5665	*Palaeoscincus* sp. (Gilmore, 1930; Matthew, 1922); *Edmontonia* sp. (Russell, 1940); *Panoplosaurus rugosidens* (Coombs, 1971): *Edmontonia* (*Chassternbergia*) sp. (Bakker, 1988); *Edmontonia rugosidens* (Burns, 2015; Carpenter, 1990).
CMN 2759*	*Panoplosaurus mirus* (Bakker, 1988; Burns, 2015; Carpenter, 1990; Coombs, 1971, 1978; Lambe, 1919; Russell, 1940; Stanford et al., 2011).
CMN 8531*	*Edmontonia longiceps* (Bakker, 1988; Burns, 2015; Carpenter, 1990; Russell, 1940; Stanford et al., 2011; Sternberg, 1928); *Panoplosaurus longiceps* (Coombs, 1971, 1978).
DMNH 468	*Edmontonia* sp. (Carpenter, 1990; Carpenter & Breithaupt, 1986); *Denversaurus schlessmani* (Bakker, 1988; Burns, 2015); *Edmontonia longiceps* (Stanford et al., 2011).
DPMWA 90-25	*Edmontonia* sp. (Gangloff, 1995); *Panoplosaurus mirus* (Burns, 2015).
ROM 1215	*Edmontonia rugosidens* (Russell, 1940); *Panoplosaurus longiceps* (Coombs, 1971, 1978); *Panoplosaurus* sp. (Bakker, 1988); *Panoplosaurus mirus* (Burns, 2015; Carpenter, 1990; Stanford et al., 2011).
ROM 20892	*Panoplosaurus longiceps* (Coombs, 1971, who used the field number ROM 2-1935); *Edmontonia* sp. 1 affin. *longiceps* (Bakker, 1988, mistakenly called ROM 1794); Panoplosaurinae *incertae sedis* (Burns, 2015).
USNM 11868*	*Palaeoscincus rugosidens* (Gilmore, 1930); *Edmontonia rugosidens* (Burns, 2015; Carpenter, 1990; Russell, 1940; Stanford et al., 2011); *Panoplosaurus rugosidens* (Coombs, 1971, 1978); *Edmontonia* (*Chassternbergia*) *rugosidens* (Bakker, 1988).

referable to *Panoplosaurus* and *Edmontonia*. In the paper on ankylosaur systematics that followed, Coombs (1978) regarded *Edmontonia* as a junior synonym of *Panoplosaurus* but did not provide his evidence for doing so. This evidence had been provided, however, in Coombs (1971), which displayed a series of plots showing different skull proportions across *Panoplosaurus* and *Edmontonia*. The results were described as "conflicting and confusing" (Coombs, 1971:87): for some parameters, the holotype skulls for *Pan. mirus* (CMN 2759) and *Ed. longiceps* (CMN 8531) were separated from those referable to *Ed. rugosidens*, suggesting that three distinct species were represented; for others, the skulls fell along a trendline that could instead be interpreted as individual variation within a single species. Coombs (1971) was not convinced that the specimens pertained to one species and considered all three species as valid. However, he argued that continuing to recognize two distinct genera was unjustified, and all the specimens were referred to *Panoplosaurus* with three recognized species, *Pan. mirus*, *Pan. longiceps*, and *Pan. rugosidens* (Coombs, 1971, 1978).

The revision of *Panoplosaurus* and *Edmontonia* by Coombs (1971, 1978) was more conservative than those that followed, particularly that of Bakker (1988) in which nearly every specimen examined was assigned to a distinct taxon. A short and "plump" snout was observed by Bakker (1988) in both the holotype of *Pan. mirus* (CMN 2759) and ROM 1215 (originally referred to *Ed. rugosidens* by Russell [1940]), although the trait is less pronounced in the latter. As such, ROM 1215 was assigned to *Panoplosaurus* as a new, but unnamed, species (Bakker, 1988). *Edmontonia longiceps* was regarded as valid by Bakker (1988), but he argued that the greatly expanded postorbital boss and shortened snout in *Ed. rugosidens* warranted a subgeneric separation and renamed it *Edmontonia* (*Chassternbergia*) *rugosidens*. Shortly after, the subgenus *Chassternbergia* was rejected by Carpenter (1990), stating that the wide palate and divergent tooth rows in *Ed. rugosidens* made the degree of snout shortening relative to *Ed. longiceps* appear greater than it is. Further, he argued that the development of the postorbital boss is subject to individual, rather than taxonomic, variation (Carpenter, 1990). Bakker's (1988) referral of ROM 1215 to *Panoplosaurus* was accepted by Carpenter (1990), although he considered it an example of *Pan. mirus* rather than a separate species. This assignment was based, in part, on a snout that tapers when viewed dorsally and "lumpy" caputegulae, which contrasted with the parallel- (or near parallel-) sided snout and smooth caputegulae observed in *Edmontonia* (Carpenter, 1990). Carpenter's (1990) revision remains well accepted and harkens back to that of Russell (1940), in which the validity of two genera and three species (*Pan. mirus*, *Ed. longiceps*, and *Ed. rugosidens*) is recognized.

In addition to caputegulal texture and snout shape, Carpenter (1990) separated *Panoplosaurus* and *Edmontonia* by differences in vomer morphology. In both *Ed. longiceps* and *Ed. rugosidens*, the paired vomers form a keel along the ventral margin, whereas in *Pan. mirus* the vomers are grooved along the midline and laterally swollen (Carpenter, 1990). This difference was considered diagnostic at the genus level, and vomer morphology has been used by other workers in referring specimens to either *Panoplosaurus* or *Edmontonia* (Burns, 2015; Carpenter, 1990; Carpenter & Breithaupt, 1986; Gangloff, 1995, Kuca, 2004). Palatal morphology was also incorporated into the revision of Bakker (1988), who considered a foramen on the medial surface of the ectopterygoid as diagnostic for *Panoplosaurus*. Further, the internal anatomy of *Pan. mirus* has frequently been referenced in the literature (Bourke et al., 2018; Kuzmin et al., 2020; Miyashita et al., 2011; Ősi et al., 2014; Paulina-Carabajal et al., 2016; Paulina-Carabajal et al., 2018; Schade et al., 2022). This has stemmed from Witmer and Ridgley's (2008) investigation into the nasal cavities of ankylosaurs, for which CT-based endocasts of the brain and nasal passages were created for *Panoplosaurus*, although only the latter was described. The findings of Bakker (1988), Carpenter (1990), and Witmer and Ridgley (2008) are problematic in the context of the taxonomic question, however, because they are based on ROM 1215 rather than CMN 2759, the holotype of *Pan. mirus*. Although referred to *Panoplosaurus* by both Bakker (1988) and Carpenter (1990), historically there has been little consensus on the taxonomy of ROM 1215, a situation typical of specimens referable to *Panoplosaurus* and *Edmontonia* (Table 1). Not only does this create uncertainty about whether ROM 1215 truly reflects the palatal and endocranial morphology of *Pan. mirus*, but also underscores the challenges in studying the cranial anatomy of CMN 2759: the complete articulation of the skull means that most cranial elements, including those of the palate, are inaccessible and have not been described. Fortunately, the advent of computed tomography (CT) scanning in paleontological research has provided an avenue for expanding on Lambe's (1919) original description of CMN 2759. Based on CT-scan data, the present work investigates previously unknown cranial elements that will supplement the formal description of *Pan. mirus*. We further affirm the taxonomic distinctiveness of *Panoplosaurus* and *Edmontonia* and provide updated diagnoses for each, based on new data presented here. The co-existence of the two nodosaurid genera may have interesting implications for megaherbivore paleoecology, discussed below.

We do not address the validity of the late Maastrichtian *Denversaurus schlessmani* (Bakker, 1988), originally referred to *Edmontonia* (Carpenter & Breithaupt, 1986), which is outside the scope of our study, limited as it is to pre-Lancian taxa.

MATERIALS AND METHODS

Materials

The holotype specimen of *Pan*. *mirus*, CMN 2759, includes a complete and fully articulated skull and partial postcranium. The specimen was collected in 1917 by C.M. Sternberg from the lower Dinosaur Park Formation, 4.4 km south of the mouth of Little Sandhill Creek, in what is now Dinosaur Provincial Park, Alberta, Canada (Arbour et al., 2009; Lambe, 1919). Lawrence Lambe (1919) erected the new genus and species, *Pan. mirus*, in a publication describing the skull, teeth, and dermal ossifications of CMN 2759. Unfortunately, Lambe died shortly after and was unable to complete his description of the holotype specimen, and the postcranium of CMN 2759 was described by Sternberg (1921) in a supplementary publication. The present work supplements not only that of Lambe (1919), but also contributes to prior discussions of the comparative cranial morphology of *Panoplosaurus* and *Edmontonia* (Bakker, 1988; Burns, 2015; Carpenter, 1990; Coombs, 1971; Stanford et al., 2011). As such, previously unknown cranial elements of CMN 2759 are described and the cranial ornamentation is re-examined and compared across specimens of both *Panoplosaurus* and *Edmontonia*. The postcranium of CMN 2759 was not examined as part of the present work but has been thoroughly described elsewhere (Burns, 2015; Carpenter, 1990; Sternberg, 1921).

Methods

The skull of CMN 2759 was CT scanned on 25 March 2021, at the Jesse Garant Metrology Center (Windsor, Ontario) using a M3A Linac (3 MeV) system with a 1 mm pixel pitch panel, resulting in a stack of 1459 slices in DICOM format with isotropic voxel size of 0.5479227 mm. The raw scan data are freely available from MorphoSource (https://doi.org/10.17602/M2/M797978). The DICOM data were uploaded into the software 3D Slicer (3D Slicer, 2019; Fedorov et al., 2012), and both cranial and endocranial elements were manually segmented and rendered into three-dimensional models using the Segment Editor module. The 3D-rendered cranial elements were then described and compared with other nodosaurid specimens that were either examined personally or from descriptions in the literature. The resulting three-dimensional models of the brain and nasal passages for CMN 2759 were compared with those of other ankylosaurs that have been described in the literature, with particular attention given to digital casts of internal cavities that have also been reconstructed from CT scan data as these have been found to provide the most thorough and accurate sources of information (Kuzmin et al., 2020; Miyashita et al., 2011; Paulina-Carabajal et al., 2016). Direct comparisons were made between the CT scan data and digital casts of internal cavities for CMN 2759 and the referred *Panoplosaurus* specimen ROM 1215; the CT scanning and data processing for ROM 1215 are described in Witmer and Ridgley (2008). Specimen measurements were taken with a Vernier caliper and measuring tape. Measurements of the internal elements in CMN 2759 were taken in 3D Slicer using the Markups module, and flexure of brain endocasts were measured in the software ImageJ (Schneider et al., 2012).

Terminology for Cranial Ornamentation—The term 'caputegulum,' meaning 'skull tile,' was first proposed by Blows (2001) for the flat bones that cover the skulls of ankylosaurs. This was done in response to the poorly defined and inconsistent terminology then being used in the literature for ankylosaur dermal ossifications (Blows, 2001). For instance, 'osteoderm' has been used to describe various types of ornamentation despite being defined as bony elements that form within the dermis and therefore distinct from those that form as outgrowths of cranial bones (Blows, 2001; Ősi et al., 2021; Vickaryous et al., 2001; Vickaryous & Sire, 2009). As such, the use of 'caputegulum' is beneficial because it makes no reference to the morphogenesis of cranial ornamentation, which has only been investigated for a small number of ankylosaur specimens (Arbour & Currie, 2013; Leahey et al., 2015; Ősi et al., 2021; Vickaryous et al., 2001). Arbour and Currie (2013) further refined the term with modifiers for identifying caputegulae by their location in ankylosaurids (e.g., nasal caputegulum), thus facilitating the comparison of cranial ornamentation patterns across taxa. These modifiers are based on the cranial anatomy of the Asian ankylosaurid *Pinacosaurus grangeri*, one of the few ankylosaur taxa for which the boundaries between cranial bones are known (Arbour & Currie, 2013; Vickaryous et al., 2004). This terminology is used here to describe the ornamentation in CMN 2759 and to assess ornamentation patterns across specimens of *Panoplosaurus* and *Edmontonia*, but with the caveat that there may not be a precise congruence between the location modifiers and the underlying cranial bones. Location modifiers have been used previously for the caputegulae in nodosaurids, but the terminology differs among workers (Kirkland et al., 2013; Lee, 1996; Stanford et al., 2011) and, unlike Arbour and Currie (2013), the modifiers were conjectural and not based on cranial bone boundaries that have been directly observed in an ankylosaur. Overlap in the terminology of Arbour and Currie (2013) with the present work is not meant to imply that the cranial ornamentation in nodosaurids and ankylosaurids is homologous, which has not been established and is beyond the scope of this paper. To reflect this, a different colour scheme to that of Arbour and Currie (2013) was chosen for identifying the distinct caputegulae in *Panoplosaurus* and *Edmontonia*. The term 'boss' is used here for the expansion of the postorbital and quadratojugal regions in *Panoplosaurus* and *Edmontonia* to distinguish them from the more prominently developed 'horns' of ankylosaurids (Arbour & Currie, 2013). These same regions were termed 'protuberances' by Carpenter (1990), but the use of 'boss' is preferred as it is an established term for knob-like structures that occur in certain animals.

Institutional Abbreviations—**AMNH**, American Museum of Natural History, New York, NY, U.S.A.; **CMN**, Canadian Museum of Nature, Ottawa, Canada; **DMNH**, Denver Museum of Nature and Science, Denver, CO, U.S.A.; **DPMWA**, Dorothy Page Museum, Wasilla, AK, U.S.A.; **FWMSH**, Fort Worth Museum of Science and History, Fort Worth, TX, U.S.A.; **IPUW**, Paläontologisches Institut der Universität, Vienna, Austria; **MPC**, Institute of Paleontology and Geology, Mongolian Academy of Sciences, Ulaanbaatar, Mongolia; **NHMUK** (formerly **BMNH**), Natural History Museum, London, U.K.; **PIN**, Paleontological Institute, Russian Academy of Sciences, Moscow, Russia; **QM**, Queensland Museum, Brisbane, Australia; **ROM**, Royal Ontario Museum, Toronto, Canada; **SMU**, Shuler Museum of Palaeontology, Southern Methodist University, Dallas, TX, U.S.A.; **TMP**, Royal Tyrrell Museum of Paleontology, Drumheller, Canada; **UALVP**, University of Alberta Laboratory for Vertebrate Palaeontology, Edmonton, Canada; **USNM**, National Museum of Natural History, Washington, DC, U.S.A.; **ZIN PH**, Paleoherpetological Collection, Zoological Institute, Russian Academy of Sciences, Saint Petersburg, Russia.

DESCRIPTION OF THE SKULL OF CMN 2759

Skull

General Comments—The holotype skull of *Pan*. *mirus* (CMN 2759; Figs. 2, 3) is well preserved and completely articulated, including lower jaws. The left buccal caputegulae are missing, but the skull is otherwise complete. The ventral rim of the left orbit is compressed dorsomedially, and the ventral ramus of the left quadrate and the left pterygoid flange are more laterally oriented relative to those of the right. In all other respects, the skull appears undistorted. Skull measurements are provided in Table 2.

Cranial Ornamentation—As noted previously (Bakker, 1988; Carpenter, 1990; Lambe, 1919), the cranial ornamentation of CMN 2759 is markedly rugose with discrete caputegulae that are separated by deep furrows. The furrows are generally shallower and less defined in *Edmontonia*, although this trait varies between *Panoplosaurus* and *Edmontonia*, depending on the state of preservation. While the postorbital bosses of CMN 2759 are covered in numerous small caputegulae, only nine cover the rest of the dorsal surface (Fig. 4). The median narial caputegulum is a large pentagonal element that extends laterally along the dorsal and posterior borders of the nares, forming a narrow wedge that lies between the nares and the anterior-most nasal caputegulae (Fig. 5). This lateral wedge of the median narial caputegulum is also observed in the referred *Panoplosaurus* specimens ROM 1215 and TMP 1983.025.0002 (Fig. 5). In *Edmontonia* and *D. schlessmani* (considered *Edmontonia* sp. by Carpenter & Breithaupt, 1986; Carpenter, 1990), the median narial caputegulum only extends as far as the medial border of the naris, and the nares and nasal caputegulae are separated by the supranarial caputegulae rather than the median narial caputegulum seen in *Panoplosaurus* (Fig. 5). Supranarial caputegulae are also preserved in the referred *Panoplosaurus* specimens TMP 1983.025.0002 and TMP 1998.067.0001, so the absence of this element in CMN 2759 may be ontogenetic or taphonomic. The nasal caputegulae consist of two rows of paired elements that form transverse bands across the muzzle in CMN 2759. The anterior pair widen as they extend laterally and then ventrally, while the posterior pair curve posteriorly along the edge of the frontoparietal caputegulum until they contact the postorbital bosses. The same arrangement of nasal caputegulae is observed in TMP 1983.025.0002 and CMN 8529 (Fig. 4). Among other specimens that have been referred to *Panoplosaurus*, a fifth nasal caputegulum (the internasal caputegulum) is located medially. The shape of the internasal caputegulum is variable (Fig. 4), appearing triangular (ROM 1215), sub-rectangular (TMP 1998.067.0001), or oval (DPMWA 90-25). Both patterns are distinguishable from *Edmontonia* and *D. schlessmanni* for which the nasal caputegulae are paired and form large rectangular or pentagonal elements (Fig. 4). The reduced number of nasal caputegulae differs from the condition observed in the Early Cretaceous nodosaurids *Pawpawsaurus campbelli* (Lee, 1996) and *Borealopelta markmitchelli* (Brown et al., 2017), in which the nasal caputegulae are numerous, small, and sub-squared. The lacrimal caputegulum in CMN 2759 lies lateral to the posterior-most nasal caputegulum, and in between the anterior nasal caputegulum and the postorbital boss. This element is also present in TMP 1983.025.0002 and ROM 1215 but cannot be discerned in TMP 1998.067.0001, DPMWA 90-25, or CMN 8529 due to poor preservation. The lacrimal caputegulae are larger in *Ed. longiceps* (CMN 8531) and *Ed. rugosidens* (USNM 11868, AMNH 5381, UALVP 16249), encroaching into the prefrontal region, and are bordered medially by the frontoparietal caputegulum rather than the nasal caputegulae as seen in *Panoplosaurus*. Lacrimal caputegulae appear to be absent in *D. schlessmanni*. The frontoparietal caputegulum is the largest dermal element in CMN 2759, accounting for nearly half of the dorsal surface. Immediately posterior to the frontoparietal caputegulum is the nuchal caputegulum, which forms a narrow transverse band across the posterior edge of the skull. Both the frontoparietal and nuchal caputegulae are similarly present in other specimens referable to *Panoplosaurus* and *Edmontonia*, as well as other nodosaurid taxa, and may have been common among these forms (Brown et al., 2017; Carpenter et al., 1999; Kirkland et al., 2013; Lee, 1996). As mentioned previously, the postorbital boss ornamentation in CMN 2759 is subdivided into several small and randomly dispersed caputegulae, a condition observed in all specimens of *Panoplosaurus* for which the postorbital bosses are preserved. This differs from the condition in *Edmontonia*, in which the postorbital bosses are covered by two caputegulae that are divided anteroposteriorly. The area between the lower jaws in CMN 2759 is completely covered ventrally by numerous gular osteoderms (Fig. 2B). Along the lateral-most extent of this ventral surface (medial to the dentaries and posterior to the predentary) is a swath of small, randomly shaped, and tightly compressed gular osteoderms. Medially and extending posteriorly, the gular osteoderms transition from small ovals to larger oblong elements that are oriented either anteroposteriorly or anterolaterally. Gular osteoderms—common to all early diverging thyreophoroids (sensu Raven et al., 2023)—also occur in AMNH 5381 (referred to *Ed. rugosidens*), which is the only other specimen from either genus for which this area is, at least partially, preserved.

Seven caputegulae of varying size and shape cover the right buccal region of CMN 2759 (Figs. 3A, 5). The most prominent buccal caputegulum is a large oblong element that shields the medially offset row of maxillary teeth. Immediately anterior is a small circular caputegulum, while posteroventrally there is a small lenticular one. Beginning at the posterodorsal edge of the large buccal caputegulum and extending posteriorly between the suborbital bar and lower jaw are another four sub-rectangular caputegulae. The buccal caputegulae are unique among the cranial ornaments in CMN 2759, in that there is no indication that they were directly fused to any skull bones (Fig. 6). The dorsoventrally compressed suborbital bar appears too thin to have supported buccal caputegulae, nor are any areas of attachment visible along the suborbital bar, quadratojugal, or lower jaw. None of the buccal caputegulae have been retained on the left side of the skull, leaving the deep buccal emargination exposed. These findings suggest that the buccal caputegulae are osteoderms that were embedded in skin. Buccal osteoderms are rarely preserved among specimens of *Panoplosaurus* and *Edmontonia*, having only been found in CMN 2759 and the referred *Ed. rugosidens* specimen AMNH 5381 (Fig. 5). The lower jaws in both CMN 2759 and AMNH 5381 are preserved in articulation, possibly increasing the likelihood that the buccal osteoderms remained in place prior to burial. Although not all the buccal osteoderms are preserved in AMNH 5381, the ones that have been retained strongly resemble those of CMN 2759, suggesting that the morphology of these elements may have been similar across both *Panoplosaurus* and *Edmontonia*.

Palatal Region—Maxillary alveoli can be discerned in the CT images of CMN 2759, which reveal the arcuate curvature of the tooth rows (Figs. 6B, 7A). From the posterior-most extent, the tooth row extends anteromedially for approximately half the length before curving anteriorly, creating a pronounced lingual bowing. This corresponds to the curvature of the tooth rows in the referred *Panoplosaurus* specimen ROM 1215, both species of *Edmontonia*, and the Early Cretaceous nodosaurid *Paw. campbelli* (Lee, 1996). The tooth rows of CMN 2759 and *Ed. rugosidens* are widely divergent relative to those of *Ed. longiceps* (Fig. 7). Lambe (1919) provided a thorough description of the teeth of CMN 2759 but could only account for eight maxillary teeth, although he acknowledged that the precise number of teeth was unknown. The CT imagery for CMN 2759 shows that there were approximately 16 maxillary alveoli, which is the same number reported in both species of *Edmontonia* (Gilmore, 1930; Sternberg, 1928).

While the vomers are identifiable in the CT images of CMN 2759, the resolution is insufficient for generating a 3D model. However, comparisons between the CT images of CMN 2759

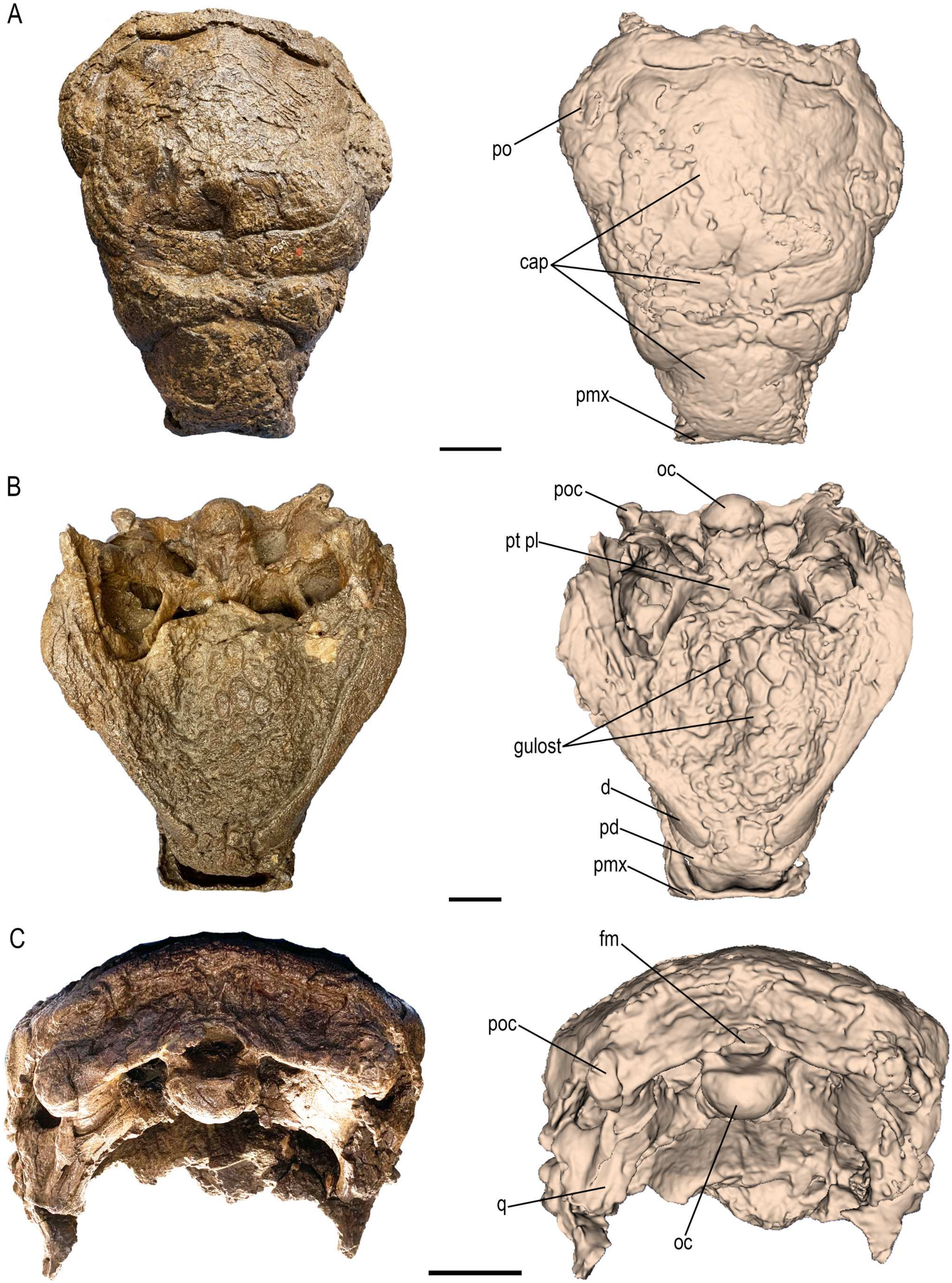

FIGURE 2. Skull of *Panoplosaurus mirus* CMN 2759 (left) and corresponding CT-based models (right). **A**, dorsal view; **B**, ventral view; **C**, posterior view. **Abbreviations**: **cap**, caputegulum; **d**, dentary; **fm**, foramen magnum; **gulost**, gular osteoderm; **oc**, occipital condyle; **pd**, predentary; **pmx**, premaxilla; **po**, postorbital boss; **poc**, paraoccipital process; **pt pl**, pterygoid plate; **q**, quadrate. Scale bars equal 5 cm.

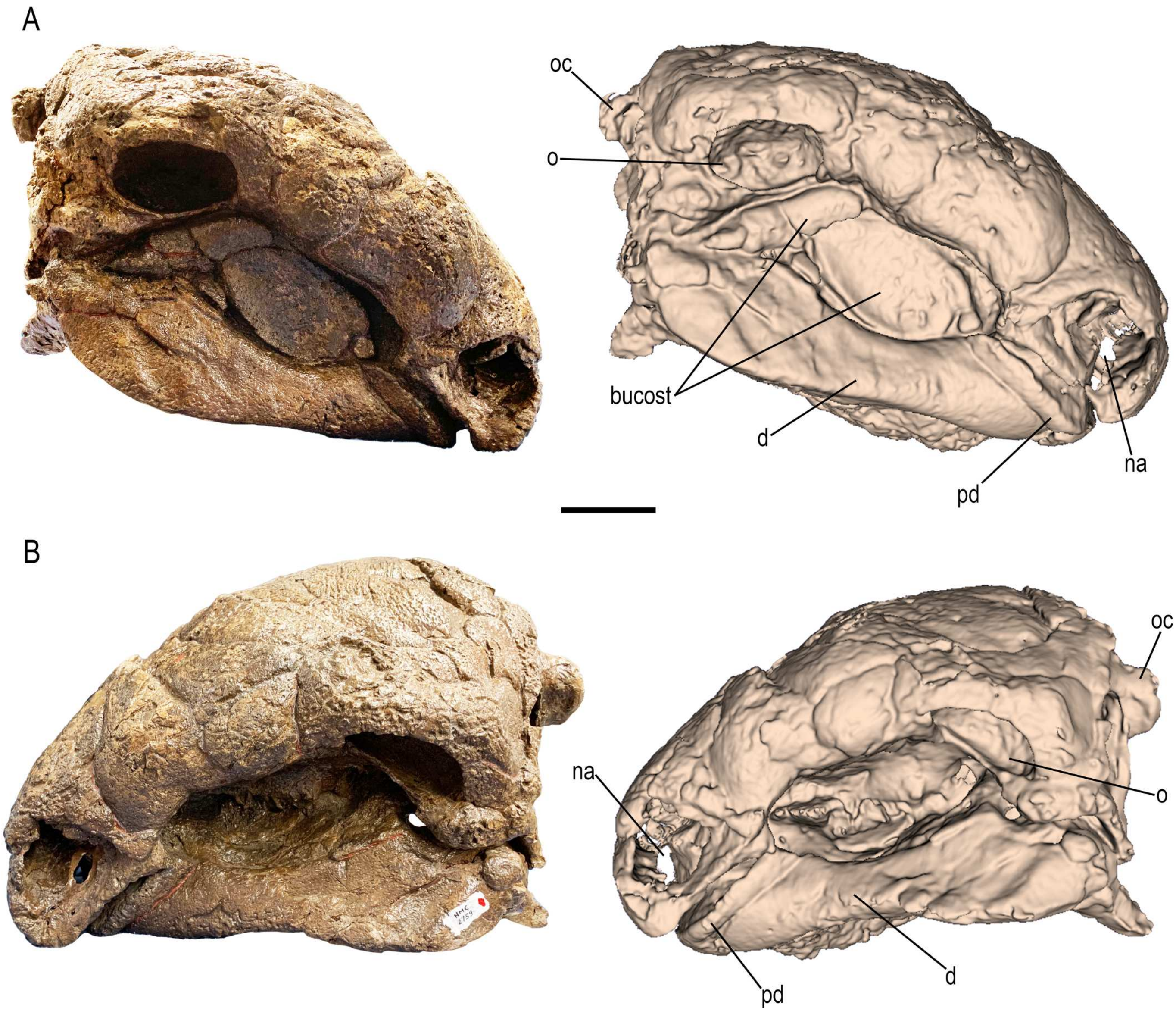

FIGURE 3. Skull of *Panoplosaurus mirus* CMN 2759 and corresponding CT-based models. **A**, right lateral view; **B**, left lateral view. **Abbreviations**: **bucost**, buccal osteoderm; **d**, dentary; **na**, naris; **o**, orbit; **oc**, occipital condyle; **pd**, predentary. Scale bars equal 5 cm.

and those of the referred *Panoplosaurus* specimen ROM 1215 demonstrate a similar vomer morphology in which the originally paired vomers fuse along the midline into a median septum with an expanded and distinctive ventral shape (Fig. 8). In the CT image (horizontal orientation), the vomers are lenticular to tear-drop shaped and hollowed internally, forming a tube-like structure. At the ventral-most end of the vomers in the CT images, the anterior contact forms a sharp point that becomes rounded to squared as the vomers extend dorsally. The inverse trend is observed at the posterior contact. The hollowed structure formed by the vomers is also visible in axial orientation, although they are not as well defined in the CT images for CMN 2759 as in ROM 1215. Despite this, the cylindrical outline of the vomers in CMN 2759 indicates that they have the same lateral expansion as those of ROM 1215. Ventrally, the vomers in ROM 1215 curve in toward each other, enclosing the hollowed space in a complete tube, but remain unfused ventrally, creating the deep longitudinal groove that has been described by previous workers (Burns, 2015; Carpenter, 1990; Russell, 1940; Fig. 8F). A cylindrical structure shaped by the medially curving vomers also occurs in the referred *Panoplosaurus* specimen TMP 1983.025.0002 (Fig. 8E), but the vomers are closed rather than deeply grooved as observed in ROM 1215. It is currently unknown whether there is a hollow median space between the vomers in TMP 1983.025.0002. The scan data for CMN 2759 are not absolutely definitive, but the groove observed in ROM 1215 seems to be absent as there is bone surrounding the median hollow ventrally, suggesting that the ventral contact between the vomers is complete, perhaps similar to that of TMP 1983.025.0002. Despite these differences, the vomer morphology observed in CMN 2759, ROM 1215, and TMP 1983.025.0002 is dramatically distinct from the keeled vomers of *Edmontonia* and *D. schlessmanni* (Burns, 2015; Carpenter, 1990; Carpenter & Breithaupt, 1986; Gilmore, 1930; Sternberg, 1928). The vomers in the referred *Ed. rugosidens* specimen TMP 1991.036.0507 are partially fractured, exposing a bony interior rather than a hollow medial space. Likewise, CT scans of AMNH 5381 (referred to *Ed. rugosidens*) show no

TABLE 2. Cranial measurements (mm) for specimens of *Panoplosaurus*, *Edmontonia*, and *Denversaurus*. Measurements for DMNH 468 and USNM 11868 taken from the literature (Burns, 2015; Carpenter & Breithaupt, 1986; Gilmore, 1930). Holotype specimens are denoted by an asterisk. Basal skull length is from the tip of the premaxillae to the occipital condyle. **Abbreviations**: **Ant**., anterior; **fm**, foramen magnum; **oc**, occipital condyle; **po**, postorbital boss; **poc**, paraoccipital processes.

Specimen	Basal skull length	Skull width across po	Skull width across nasals	Ant. width across snout	Width across poc	oc height	oc width	fm height	fm width
Panoplosaurus mirus									
CMN 2759*	350	284	120	111	206	40	57	26	38
ROM 1215	411	312	173	104	213	42	42	27	38
TMP 1983.025.0002	445	290	145	143	?	48	54	?	?
TMP 1998.067.0001	500	325	120	?	?	?	?	?	?
Edmontonia longiceps									
CMN 8531*	440	310	179	118	170	48	57	32	27
Edmontonia rugosidens									
USNM 11868*	455	332	167	133	204	42	59	?	?
AMNH 5381	416	366	158	120	280	52	61	47	39
Edmontonia sp.									
TMP 1991.036.0507	460	360	175	?	246	76	52	?	?
TMP 2000.012.0158	535	334	128	150	230	49	51	?	?
Denversaurus schlessmanni									
DMNH 468*	488	220	191	129	268	59	69	42	36

ventral vomerine groove, and any internal cavity is subtle and of minimal extent at best. Unfortunately, the relevant ventral-most part of the vomer in the holotype of *Ed. rugosidens* (USNM 11868) is largely broken away and missing (and has been since Gilmore's, 1930 time), so this trait cannot be checked throughout the full length of the bone; CT scans, however, show that the preserved anterior portion has neither a ventral groove nor an internal cavity and thus is consistent with AMNH 5381.

The left ectopterygoid is more complete than the right in CMN 2759 and forms the same thickened anteromedially curving pad seen in other specimens of *Panoplosaurus* and *Edmontonia*. There is a foramen on the medial surface of the left ectopterygoid in CMN 2759 and, although incomplete, it appears to be mirrored on the right side (Fig. 9B). The position of the ectopterygoid foramen is identical to that of the referred *Panoplosaurus* specimen ROM 1215 and was suggested by Bakker (1988) to have accommodated the ascending branch of the palatine artery. Porter and Witmer (2020) tracked a similar foramen in ankylosaurids (and other archosaurs) that corresponds to a highly reduced suborbital fenestra and transmitted the palatine artery and vein after branching from the palatomaxillary vessels; although ankylosaurids retain a small suborbital foramen between the ectopterygoid, palatine, and maxillary bones, it is possible that the foramen was captured by the ectopterygoid in whole or part in various nodosaur specimens. For example, in *Ed. longiceps* (CMN 8531), there is a possible foramen on the medial surface of the left ectopterygoid that would correspond to that of CMN 2759 and ROM 1215, while in the referred *Panoplosaurus* specimen ROM 20892, the foramen is located on the anteroventral surface of the ectopterygoid. We observed no ectopterygoid foramina in other examined specimens, although ankylosaurs have apomorphically small palatine vessels (Porter & Witmer, 2020), and we cannot dismiss the possibility that the corresponding foramina were missed or otherwise adjacent to the ectopterygoid. Posteriorly, the ectopterygoids are fused with the anterior terminus of the pterygoid flanges, which project anterolaterally and are mediolaterally compressed with a slight ventrolateral tilt. When viewed ventrally, the pterygoids form the complex W-shaped structure commonly observed in ankylosaurs (Vickaryous et al., 2004), with a transversely broad pterygoid plate having a slight anterodorsal projection. A blunt medial ridge extends anteroposteriorly along the ventral surface, marking the contact between the paired pterygoids. This medial ridge forms a prominent and sharp-edged keel in referred specimens of *Panoplosaurus* and *Edmontonia*, and the relatively blunted ridge in CMN 2759 may be due to taphonomic degradation, as the region is exposed in this specimen. The posterior surface of the pterygoid plate contacts the basisphenoid and the basipterygoid processes. This surface is damaged in CMN 2759, but it is likely to have had the same thickened triangular to lenticular medial process that is present in other specimens of *Panoplosaurus* and *Edmontonia*.

Basicranium—The elements comprising the basicranium are tightly fused and form a robust structure that projects posteroventrally when the skull is positioned horizontally (Fig. 9). There is no evidence of sutures in either the original specimen or the CT images, so the contact between individual bones cannot be distinguished with any precision. The foramen magnum is oval and bordered by the supraoccipital dorsally, the otoccipitals laterally, and the basioccipital ventrally. However, the extent to which each element contributes to the margin of the foramen magnum cannot be determined with any certainty.

The anterior-most extent of the nuchal crest is preserved in CMN 2759 and marks the midline of the supraoccipital. The posteromedial portion of the supraoccipital is missing, but what remains forms an awning-like edge that overhangs the dorsolateral corners of the foramen magnum, forming facets for articulation with the proatlas. The supraoccipital is notched at the approximate midpoint between the lateral-most extent and the midline of the protruding edge, giving it a scalloped appearance when viewed dorsally. Similar scalloping is observed in other specimens of *Panoplosaurus* and *Edmontonia* and appears to have been consistent across both genera. Anterior to these notches in CMN 2759 are foramina (one on the right of the midline and two smaller ones on the left) that pierce the foramen magnum dorsolaterally. Similarly placed foramina occur in the basally branching nodosaurid *Paw. campbelli* and basally branching ankylosaurid *Bissektipelta archibaldi*, and were attributed to small supraoccipital veins in the latter (Kuzmin et al., 2020; Lee, 1996). In CMN 2759, these foramina open into paired sulci that extend anteroposteriorly along the dorsolateral corners of the foramen magnum. Ventral to the sulcus on the left side is a single foramen that could, based on what is known from other ankylosaur specimens (Kuzmin et al., 2020; Paulina-Carabajal et al., 2016), correspond to the

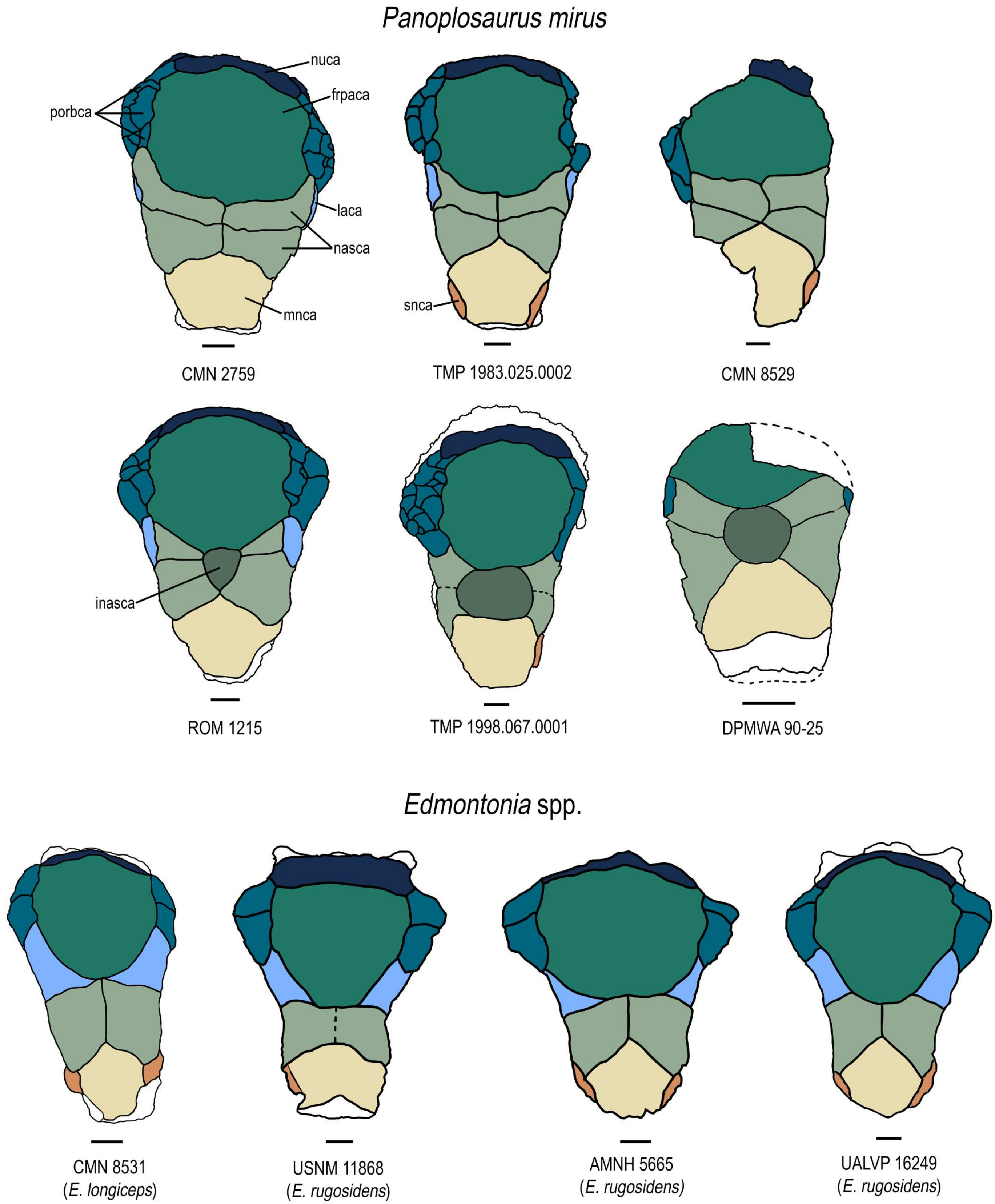

FIGURE 4. Cranial ornamentation in *Panoplosaurus* and *Edmontonia* skulls in dorsal view, with distinct caputegulae color coded for comparative purposes. Only skulls with adequate dorsal preservation have been included. The image for DPMWA 90-25 was modified from Burns (2015), USNM 11868 from Gilmore (1930), and UALVP 16249 from Kuca (2004). **Abbreviations**: **frpaca**, frontoparietal caputegulum; **inasca**, internasal caputegulum; **laca**, lacrimal caputegulum; **mnca**, median narial caputegulum; **nasca**, nasal caputegulum; **nuca**, nuchal caputegulum; **porbca**, postorbital caputegulum; **snca**, supranarial caputegulum. Images scaled to uniform anteroposterior length. Scale bars equal 5 cm.

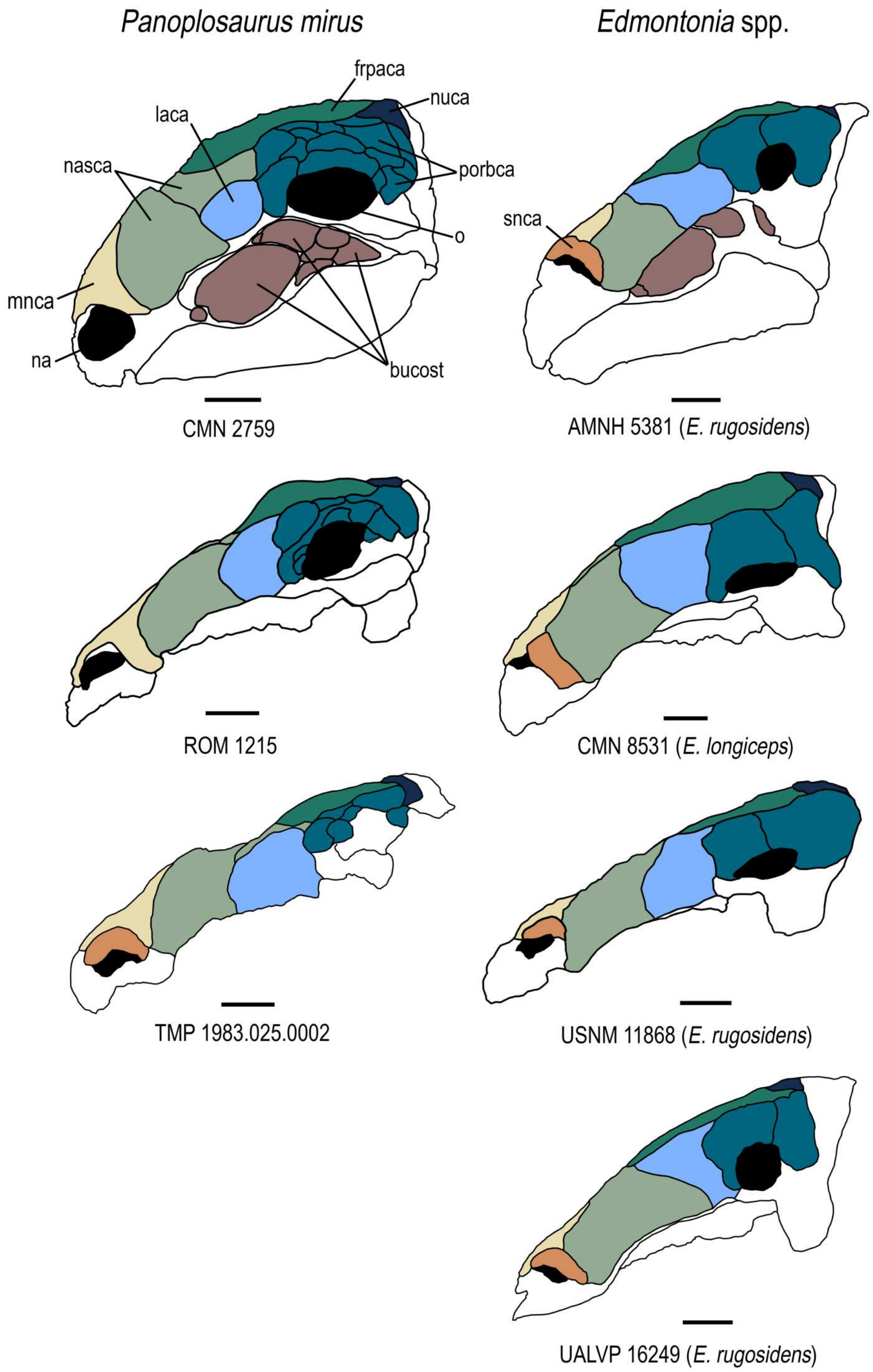

FIGURE 5. Cranial ornamentation in *Panoplosaurus* and *Edmontonia* skulls in left lateral view, including in situ buccal osteoderms (CMN 2759, AMNH 5381). Distinct caputegulae are color coded for comparative purposes. Only skulls with adequate lateral preservation have been included. The images for CMN 2759 and AMNH 5381 are reversed. The image for USNM 11868 was modified from Burns (2015). **Abbreviations**: **bucost**, buccal osteoderms; **frpaca**, frontoparietal caputegulum; **laca**, lacrimal caputegulum; **mnca**, median narial caputegulum; **na**, naris; **nasca**, nasal caputegulum; **nuca**, nuchal caputegulum; **o**, orbit; **porbca**, postorbital caputegulum; **snca**, supranarial caputegulum. Images scaled to uniform anteroposterior length. Scale bars equal 5 cm.

position of the hypoglossal cranial nerve (CN XII). This assignment, however, is tentative as the foramen is not mirrored on the right side nor are there any other foramina visible that could offer insight based on relative positioning.

The paired paraoccipital processes of the otoccipitals, formed from the fusion of the exoccipitals and opisthotics (Vickaryous et al., 2004), extend laterally from either side of the foramen magnum with a pronounced posteroventral orientation. They are compressed dorsoventrally relative to the anteroposterior depth, giving them a wing-like appearance. The dorsoventral thickness increases towards the lateral terminus, although this is more pronounced on the left side. The left lateral terminus is better preserved than the right and forms a thickened cap that is greatly rounded along the distal edge and more expanded dorsoventrally than anteroposteriorly. The ventral surface of the lateral terminus is completely fused with the quadrate. The triramous quadrates are transversely broad and oriented anteroventrally, contacting the paraoccipital processes dorsally, the pterygoid flanges medially, the quadratojugals laterally, and the articulars ventrally. The posterior surface is subtly convex, and the anterior surface is correspondingly concave. The mandibular condyle of the left quadrate is better preserved than that of the

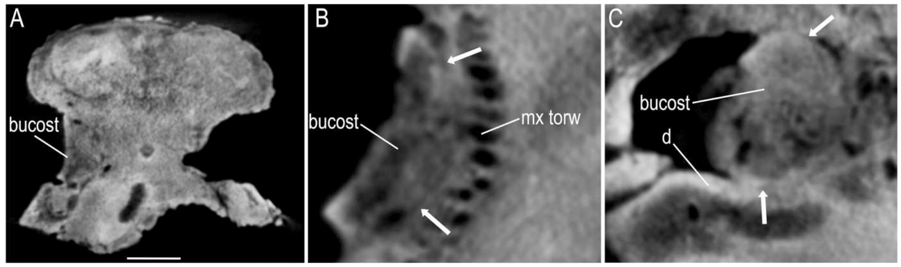

FIGURE 6. CT scan images of the right buccal osteoderm in *Panoplosaurus mirus* CMN 2759. CT slices in axial, **A**, horizontal, **B**, and parasagittal, **C**, orientation. The white arrows indicate the separation between the buccal osteoderm and other skull elements, suggesting a lack of fusion. **Abbreviations**: **bucost**, buccal osteoderm; **d**, dentary; **mx torw**, maxillary tooth row. Scale bar in **A** equals 5 cm. Images in **B** and **C** not to scale.

right and is sub-oval when viewed ventrally, with the long axis oriented mediolaterally at approximately 33° to the horizontal. The articular surface is concave, with the greatest depression situated medially and gradually shallowing towards the lateral edge. The dorsoventrally compressed pterygoid ramus of the quadrate extends medially and slightly anterodorsally and is completely fused with the pterygoid plate. When viewed laterally, the quadrate of CMN 2759 has a posterodorsal inclination of approximately 59° (measured from the horizontal as the skull sits on a flat surface). Among the few specimens for which this character can be measured, this inclination is closer to that of *Ed. longiceps* (CMN 8531, 56°) and *Ed. rugosidens* (USNM 11868, 52°; UALVP 16249, 53°) than to the referred *Panoplosaurus* specimen ROM 1215 (36°). This character is difficult to assess in *Panoplosaurus* and *Edmontonia* (and ankylosaurs in general; Vickaryous et al., 2004), as many skulls have undergone some degree of distortion that affects the orientation of the quadrates. Whether variation in quadrate inclination reflects genuine morphology or taphonomic processes remains uncertain.

The occipital condyle in CMN 2759 is reniform with the greatest curvature along the ventral surface. The occipital condyle is spherical in other specimens of *Panoplosaurus*, as well as in *Edmontonia*. A spherical condyle is considered typical of nodosaurids, while a reniform or oval condyle is the condition commonly observed in ankylosaurids (Kuzmin et al., 2020). There is a well-defined rim that rings the strongly convex articular surface, separating the condyle from the very stout neck. The dorsal surface of the basioccipital is slightly depressed as it extends anteriorly toward the opening of the foramen magnum. Ventrally, the basioccipital extends anterodorsally before curving anteriorly toward the basisphenoid and pterygoids. There is a shallow and narrow longitudinal depression located medially on the basioccipital that separates the paired basal tubera, which form subtle longitudinally elongate convexities with a slight anterolateral orientation (Fig. 10A). Similar basal tubera occur in the referred *Panoplosaurus* specimens ROM 1215 and ROM 20892, although the anterolateral orientation is more pronounced than in CMN 2759. A median depression on the ventral surface of the basioccipital was also described by Gilmore (1930) in the *Ed. rugosidens* holotype, USNM 11868. In *Ed. longiceps* (CMN 8531) and the referred *Ed. rugosidens* specimens AMNH 5381 and TMP 1991.036.0507, the basal tubera are separated medially by a ridge instead of a depression (Fig. 10B). Differing from both *Panoplosaurus* and *Ed. rugosidens*, the basal tubera in *Ed. longiceps* (CMN 8531) extend anteromedially rather than anterolaterally. In both genera, the basal tubera are less prominent than the bulbous tuberosities observed in other nodosaurids, such as *Paw. campbelli* (Lee, 1996), *Struthiosaurus austriacus* (Pereda Suberbiola & Galton, 2001), *Hungarosaurus* sp. (Ősi et al., 2014), and particularly *Niobrarasaurus coleii* (Carpenter & Everhart, 2007). Although there is damage to the right side, there are paired oblong protuberances immediately anterior to the basal tubera in CMN 2759 that extend anteromedially toward the posterior surface of the pterygoids. The general morphology and position suggest that these are the basipterygoid processes. The anterior surface of the basisphenoid and other elements of the braincase are not discernible in CMN 2759.

Endocranium

Brain Endocast—The endocast of CMN 2759 is digitally reconstructed from CT scan data with each neural region (forebrain, midbrain, hindbrain) represented, as well as cavities for the olfactory tract, olfactory bulbs, pituitary body, and internal carotid arteries (Figs. 11, 12). Due to the low density differential between the fossil and rock matrix in the CT scan, more delicate structures, such as the cranial nerves, vasculature, and endosseous labyrinths, are not visible. It is also likely that the brain did not closely fit the braincase in CMN 2759, and the resulting endocast thus does not faithfully reflect the structure of the brain proper. This would correspond to findings in other ankylosaurs, such as *Paw. campbelli* (Paulina-Carabajal et al., 2016), *S. austriacus* (Schade et al., 2022), *Hungarosaurus* sp. (Ősi et al., 2014), *Euoplocephalus tutus* (Miyashita et al., 2011), and *B. archibaldi* (Kuzmin et al., 2020). Research into the brain-endocast correspondence in extant archosaurs has shown that even in cases of relatively low brain-braincase fidelity (e.g., *Alligator mississippiensis*), endocasts provide a reliable proxy for brain morphology in relatively young/small sizes (Watanabe et al., 2019), but the endocasts become progressively less brain-like as they approach adult body size (Hu et al., 2021). Based on size, CMN 2759 can be regarded as an adult, and assuming a more crocodile-like allometry, the endocast likely did not strongly reflect brain morphology. Given these caveats, the gross morphology of the brain in *Pan. mirus* is provided below.

When viewed laterally, the brain endocast of CMN 2759 is relatively elongate and dorsoventrally narrow, and most closely resembles that of the Asian ankylosaurid *Talarurus plicatospineus* (Paulina-Carabajal et al., 2018) although CMN 2759 is more sigmoidal in aspect. The endocast of CMN 2759 is only modestly dorsoventrally expanded and not as globose as those of the nodosaurids *Paw. campbelli* (Paulina-Carabajal et al., 2016), *Struthiosaurus transylvanicus* (Pereda Suberbiola & Galton, 1994), *Hungarosaurus* sp. (Ősi et al., 2014), and the "polacanthine" nodosaurid cf. *Polacanthus foxii* (Norman & Faiers, 1996). The forebrain, midbrain, and hindbrain are subtly sigmoidal in lateral view, with cerebral and pontine flexures of approximately 21° and 38°, respectively. Both the cerebral and pontine flexures are similar to those of the referred *Panoplosaurus* specimen ROM 1215 (Table 3). An unpublished endocast (courtesy of LMW) from the referred *Ed. rugosidens* specimen AMNH 5381 has a higher cerebral flexure and lower pontine flexure than either *Panoplosaurus* specimen. Relative to CMN 2759, ROM 1215, and AMNH 5381, the cerebral flexure is greater in *Paw. campbelli*, cf. *Po. foxii*, and *S. transylvanicus*, while the pontine flexure is greater in both species of

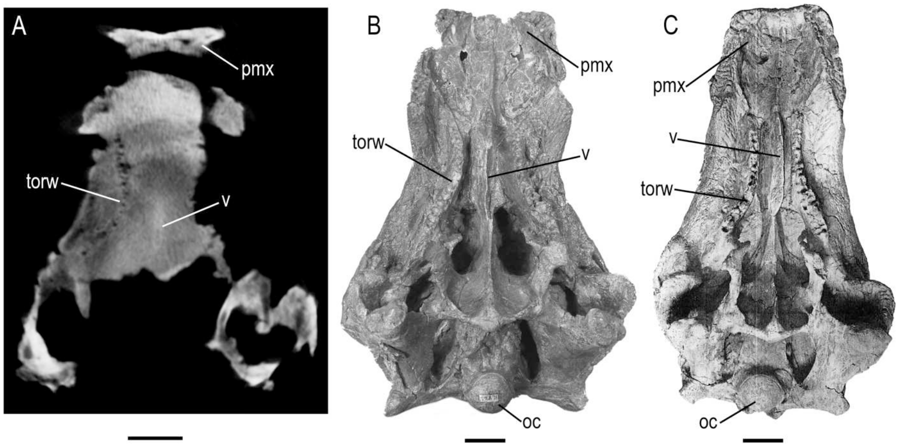

FIGURE 7. Maxillary tooth rows in the *Panoplosaurus* and *Edmontonia* spp. holotypes. **A**, CT scan slice for *Panoplosaurus mirus* CMN 2759 in horizontal orientation; **B**, *Edmontonia rugosidens* USNM 11868; **C**, *Edmontonia longiceps* CMN 8531 (modified from Sternberg [1928]) in palatal view. **Abbreviations**: **oc**, occipital condyle; **pmx**, premaxilla; **torw**, tooth row; **v**, vomers. Scale bars equal 5 cm.

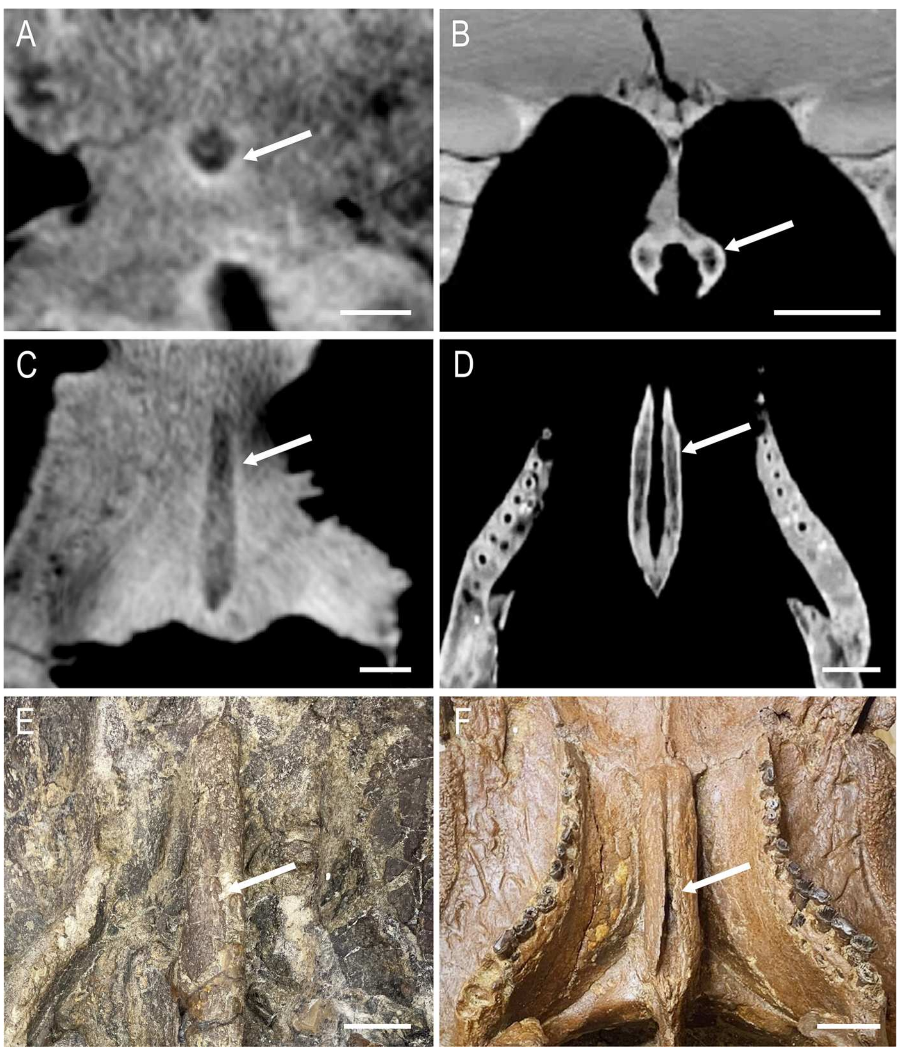

FIGURE 8. Vomer morphology in specimens of *Panoplosaurus*. CT scan images for CMN 2759, **A**, **C**, and ROM 1215, **B**, **D**, in axial, **A**, **B**, and horizontal, **C**, **D**, orientations. Palatal view of exposed vomers: **E**, TMP 1983.025.0002; **F**, ROM 1215. Vomers indicated by the white arrows. Scale bars equal 2 cm.

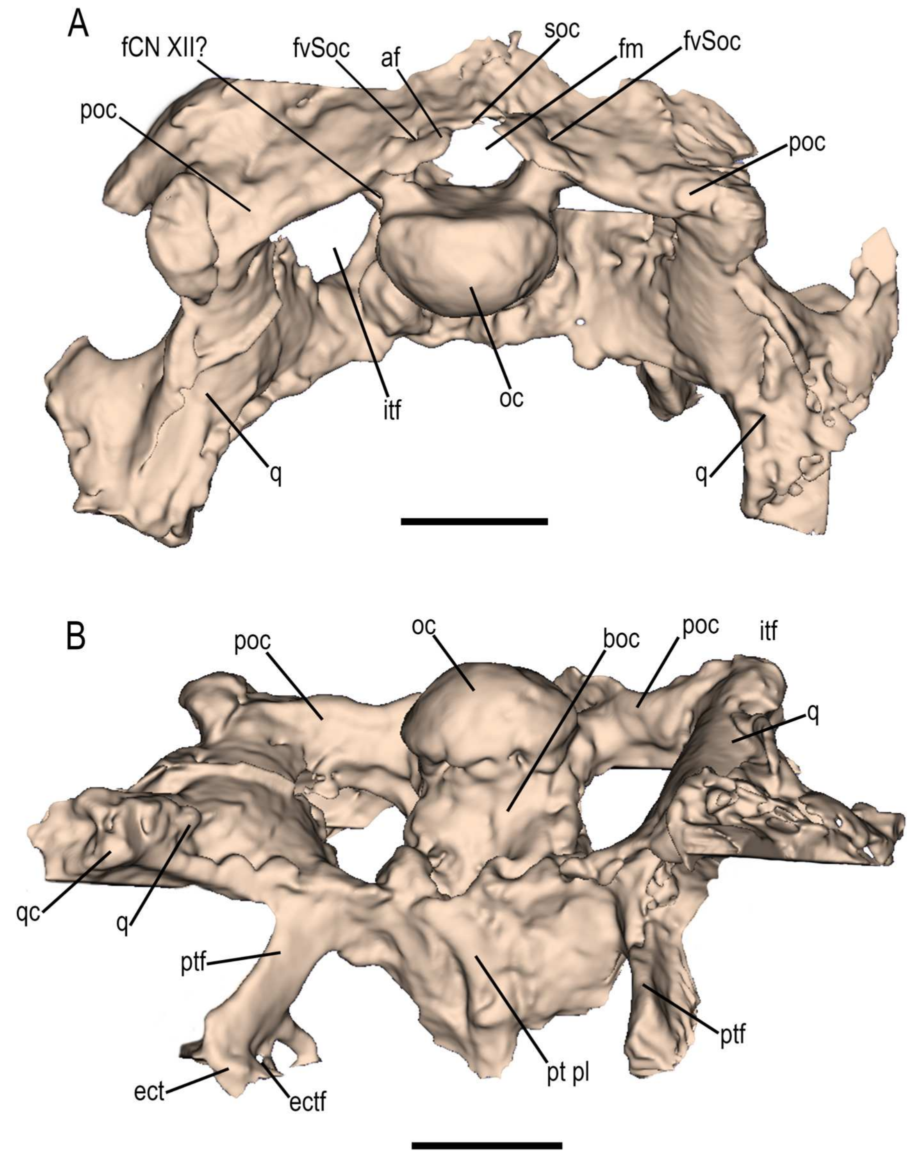

FIGURE 9. CT-based model of the basicranium in *Panoplosaurus mirus* CMN 2759. **A**, posterior view; **B**, ventral view. **Abbreviations**: **af**, atlas facet; **boc**, basioccipital; **ect**, ectopterygoid; **ectf**, ectopterygoid foramen; **fCN**, cranial nerve foramen; **fm**, foramen magnum; **fvSoc**, foramen for supraoccipital vein; **itf**, infratemporal fenestra; **oc**, occipital condyle; **poc**, paraoccipital process; **ptf**, pterygoid flange; **pt pl**, pterygoid plate; **q**, quadrate; **qc**, quadrate condyle; **soc**, supraoccipital. Scale bars equal 5 cm.

Struthiosaurus and *Hungarosaurus* sp. From the olfactory bulb cavities to the foramen magnum, the endocast in CMN 2759 measures approximately 113 mm and comprises 32% of the overall skull length. This lends support to the observation of Paulina-Carabajal et al. (2016) that nodosaurids may be distinguishable from ankylosaurids (*Eu. tutus*, 25%) and parankylosaurs (*Kunbarrasaurus ieversi*, 40%) by having brains that represent approximately 30% of the overall skull length (*Paw. campbelli*, 30%; ROM 1215, 33%).

The forebrain can be identified in the endocast of CMN 2759 by the cavities for the olfactory bulbs, olfactory tract, cerebrum, and pituitary body. The reconstructed olfactory bulbs are short (7.5 mm); however, their anterior-most extent is difficult to discern in the CT data, so it is uncertain whether their absolute length is represented in the endocast. The portion of the olfactory bulbs that is visible suggests that they have the same slight ventral projection observed in the nodosaurids *Paw. campbelli* (Paulina-Carabajal et al., 2016), *Hungarosaurus* sp. (Ősi et al., 2014), the referred *Panoplosaurus* specimen ROM 1215, and referred *Ed. rugosidens* specimen AMNH 5381. In the nodosaurid *S. transylvanicus*, the olfactory bulbs have a more pronounced ventral orientation (Pereda Suberbiola & Galton, 1994). The olfactory bulbs are oval in cross-section and diverge from the midline at an angle of 83°. Similarly divergent olfactory bulbs occur in *Paw. campbelli* (75°; Paulina-Carabajal et al., 2016), and the ankylosaurids *Eu. tutus* (80–100°; Miyashita et al., 2011) and *B. archibaldi* (80°; Kuzmin et al., 2020). The olfactory tract is anteroposteriorly short, transversely broad, and oval in cross-section. A slight depression on the dorsal surface of the olfactory tract extends posteriorly to the cerebrum, while the ventral surface is convex. An expansion immediately posterior to the olfactory tract marks the anterior-most extent of the cerebrum but lacks the pronounced cerebral expansion observed in *Paw. campbelli* (Paulina-Carabajal et al., 2016) and cf. *Po. foxii* (Norman & Faiers, 1996). The cerebrum in CMN 2759 is more expanded laterally than dorsally and gradually increases in dorsoventral thickness towards its posterior extent. The median fissure that separates the cerebrum into the paired cerebral hemispheres is not visible in CMN 2759. This is similar to other ankylosaurs and has been attributed to an enlarged longitudinal venous sinus that obscures the dorsal surface of the cerebrum (Kuzmin et al., 2020; Paulina-Carabajal et al., 2016;

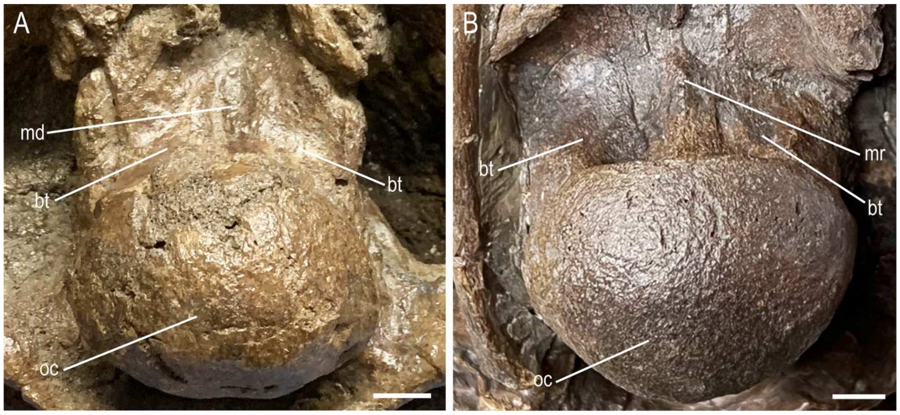

FIGURE 10. Ventral view of basal tubera separated by: **A**, a median depression in *Panoplosaurus mirus* CMN 2759; **B**, a median ridge in the referred *Edmontonia rugosidens* specimen AMNH 5381. **Abbreviations**: **bt**, basal tubera; **md**, median depression; **mr**, median ridge; **oc**, occipital condyle. Scale bars equal 1 cm.

Paulina-Carabajal et al., 2018; Witmer et al., 2008). The pituitary cavity is anteroposteriorly short, transversely wide, and projects slightly posteroventrally from the ventral surface of the endocast, similar to that observed in cf. *Po. foxii* (Norman & Faiers, 1996) and *Tal. plicatospineus* (Paulina-Carabajal et al., 2018). The pituitary cavity opens slightly anteroventrally in *S. austriacus* (Schade et al., 2022), ventrally in *Ed. rugosidens* (AMNH 5381), *Paw. campbelli* (Paulina-Carabajal et al., 2016), *B. archibaldi* (Kuzmin et al., 2020), and *Eu. tutus* (Miyashita et al., 2011), and strongly posteroventrally in *K. ieversi* (Leahey et al., 2015). The canals for the internal carotid arteries are visible at the ventral terminus of the pituitary and have a slight ventrolateral orientation.

Neural structures associated with the midbrain, such as the optic tectum, are not visible in the endocast of CMN 2759. The hindbrain, however, is indicated by the cerebellum and medulla oblongata. The cerebellum lacks the extensive dorsal expansion that occurs in the nodosaurids *S. austriacus*, *S. transylvanicus*, and *Hungarosaurus* sp. (Ősi et al., 2014; Schade et al., 2022) and is more like that of the referred *Panoplosaurus* specimen ROM 1215, referred *Ed. rugosidens* specimen AMNH 5381, *Paw. campbelli* (Paulina-Carabajal et al., 2016), and cf. *Po. foxii* (Norman & Faiers, 1996). When viewed dorsally, the cerebellum gradually narrows posteriorly and does not display the lateral expansion described for *Paw. campbelli* (Paulina-Carabajal et al., 2016). As with other nodosaurids, there is no indication of a flocculus on the lateral surface of the cerebellum (Paulina-Carabajal et al., 2016; Schade et al., 2022). Given the lack of surface detail in the endocast of CMN 2759, however, it cannot be determined whether a flocculus is truly absent. Currently, the flocculus has only been reported for the ankylosaurids *Eu. tutus* (Hopson, 1979; Miyashita et al., 2011), *Tal. plicatospineus*, and *Tarchia teresae* (Paulina-Carabajal et al., 2018). The medulla oblongata is mediolaterally wide, similar to *S. austriacus* (Schade et al., 2022) and *Paw. campbelli* (Paulina-Carabajal et al., 2016) and unlike the dorsoventrally tall medulla oblongata observed in *Hungarosaurus* sp. (Ősi et al., 2014). There is a slight medial depression on the ventral surface of the medulla oblongata. The ventral surface of the medulla oblongata is convex in *S. austriacus* (Schade et al., 2022) and flat in *Paw. campbelli* (Paulina-Carabajal et al., 2016), cf. *Po. foxii* (Norman & Faiers, 1996), and ankylosaurids (Kuzmin et al., 2020; Paulina-Carabajal et al., 2018).

Nasal Cavity—The nasal cavity is reconstructed with the respiratory region (nasal vestibules, primary nasal airways) and olfactory region identified (Figs. 11, 13). The nasal vestibules are visible as mediolaterally and dorsoventrally expanded regions that lie just inside the nares. Posterior to the nasal vestibules, two symmetrically looping nasal airways extend towards the large olfactory region. The nasal passages are medially separated throughout their entire extent, indicating the presence of the median septum. The bony or cartilaginous laminae that would have segregated the individual loops of the airway are not fully discernible, but this may well be due to the lack of contrast between fossil and matrix, which makes the CT data challenging to interpret in places. The morphology of the

TABLE 3. Cerebral and pontine flexures (measured from the long axis of the olfactory bulbs and medulla oblongata, respectively) in the endocasts of ankylosaurs. Sources provided for the flexures measured from endocasts in the literature.

Taxon		Specimen	Cerebral flexure	Pontine flexure	Source
Nodosauridae	*Panoplosaurus mirus*	CMN 2759	21º	38º	–
		ROM 1215	25º	36º	Witmer & Ridgley (2008)
	Edmontonia rugosidens	AMNH 5381	34º	26º	Unpublished endocast (courtesy of LMW)
	Pawpawsaurus campbelli	FWMSH93B.00026	44º	38º	Paulina-Carabajal et al. (2016)
	Struthiosaurus austriacus	IPUW 2349/6	?	47º	Schade et al. (2022)
	Struthiosaurus transylvanicus	NHMUK R4966	51º	57º	Ősi et al. (2014)
	Hungarosaurus sp.	PAL 2013.23.1	?	54º	Ősi et al. (2014)
	cf. *Polacanthus foxii*	CAMSM X.26242	41º	32º	Norman and Faiers (1996)
Ankylosauridae	*Euoplocephalus tutus*	AMNH 5405	22º	24º	Miyashita et al. (2011)
	Talarurus plicatospineus	MPC-D 100/1354	24º	27º	Paulina-Carabajal et al. (2018)
	Tarchia teresae	MPC-D 100/1353	?	29º	Paulina-Carabajal et al. (2018)
	Bissektipelta archibaldi	ZIN PH 1/16	30º	30º	Kuzmin et al. (2020)
Parankylosauria	*Kunbarrasaurus ieversi*	QM F18101	9º	39º	Leahey et al. (2015)

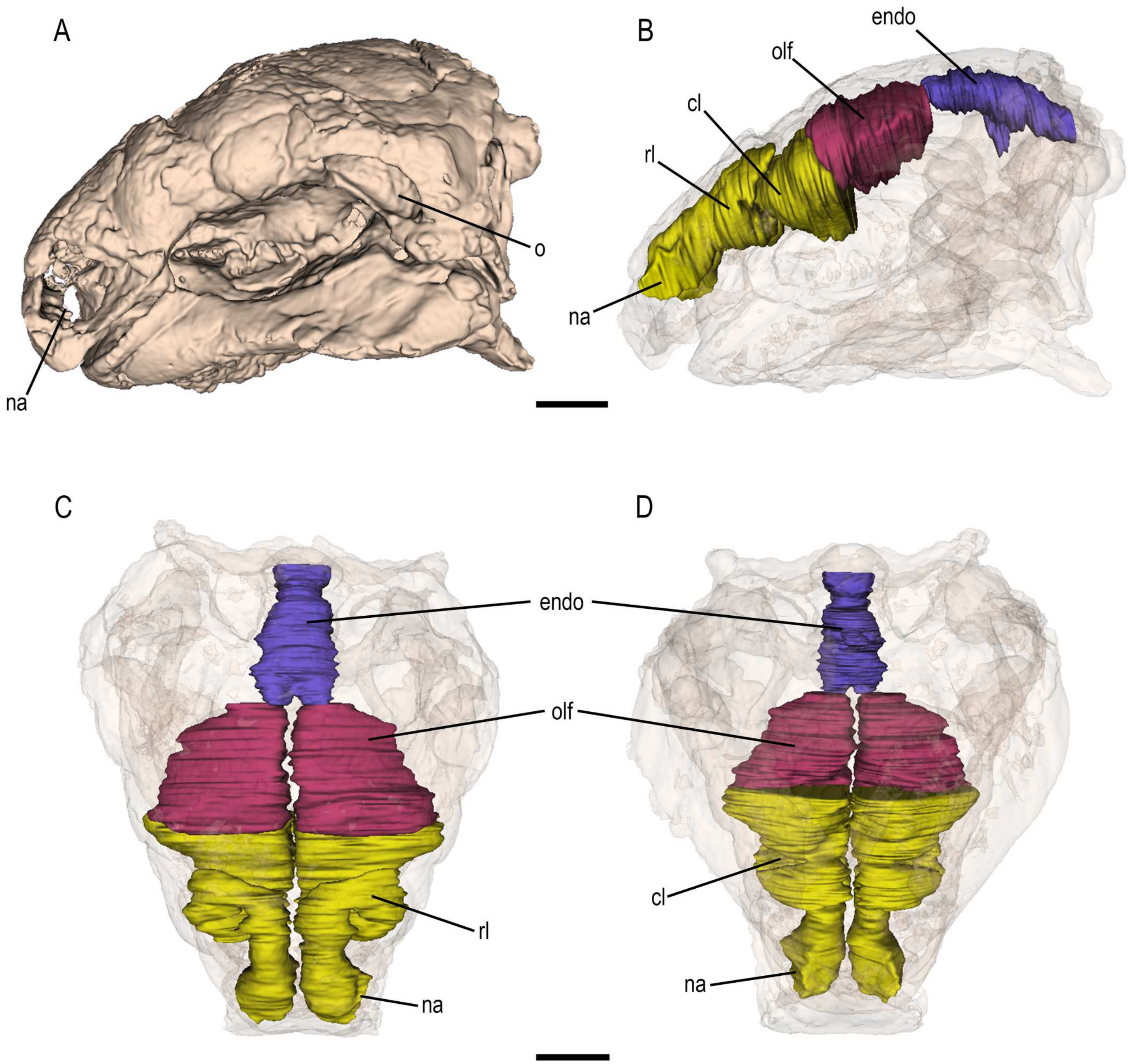

FIGURE 11. CT-based endocasts of the endocranial anatomy in *Panoplosaurus mirus* CMN 2759 including nasal passages, olfactory region, and brain (the skull is rendered semitransparent in **B**–**D**). **A**, CT rendered skull in left lateral view. Endocranial endocasts: **B**, left lateral view; **C**, dorsal view; **D**, ventral view. **Abbreviations**: **cl**, caudal loop; **endo**, endocast; **na**, naris; **o**, orbit; **olf**, olfactory region; **rl**, rostral loop. Scale bars equal 5 cm.

nasal cavity is indistinguishable from that of the referred *Panoplosaurus* specimen ROM 1215, as reconstructed and described by Witmer and Ridgley (2008), with the same distinct rostral and caudal loops. As such, the air would have taken the same convoluted route through the airway, traveling posterodorsally from the nares before turning laterally and then anteroventromedially as it continued through the anterior-most (rostral) loop (Fig. 13). Air would then travel posterodorsomedially through the posterior-most (caudal) loop before continuing posteroventrally towards the choana. Similar rostral and caudal loops have been described for the nodosaurid *Paw. campbelli*, except that the rostral loop is less laterally pronounced than that of CMN 2759 and ROM 1215, and the caudal loop is vertically rather than horizontally oriented (Paulina-Carabajal et al., 2016). Although the nasal passages in the ankylosaurid *Eu. tutus* also consist of rostral and caudal loops, the rostral loop is further subdivided resulting in a far more convoluted airway than occurs in either *Pan. mirus* or *Paw. campbelli* (Witmer & Ridgley, 2008). The precise course of the airway through the nasal cavity in the parankylosaur *K. ieversi* could not be resolved, but the presence of a nasal basin and partial partitioning observed within the nasal cavity suggest that at least some degree of complexity was present (Leahey et al., 2015). Preliminary research indicates the ankylosaurid *Tar. teresae* also possessed highly convoluted nasal passages (Tumanova et al., 2025). Immediately posterior to the respiratory region in CMN 2759 is the large olfactory region that would have contained

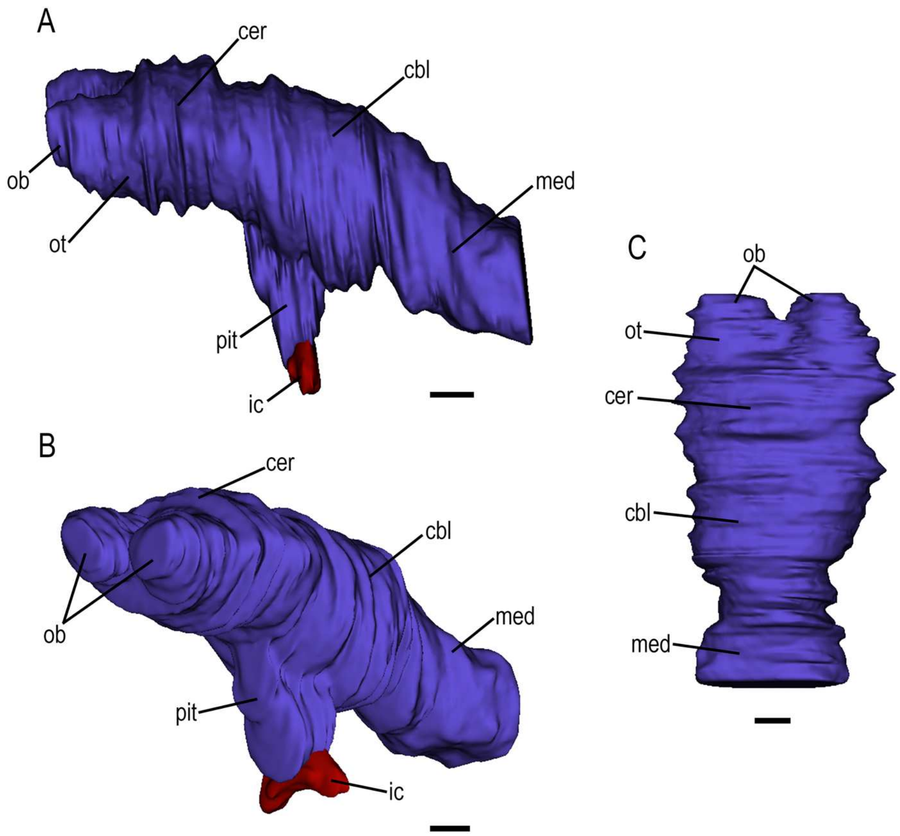

FIGURE 12. CT-based brain endocast of *Panoplosaurus mirus* CMN 2759. **A**, left lateral view; **B**, left anterolateral view; **C**, dorsal view. **Abbreviations**: **cbl**, cerebellum; **cer**, cerebrum; **ic**, internal carotid arteries; **med**, medulla oblongata; **ob**, olfactory bulbs; **ot**, olfactory tract; **pit**, pituitary. Scale bars equal 1 cm.

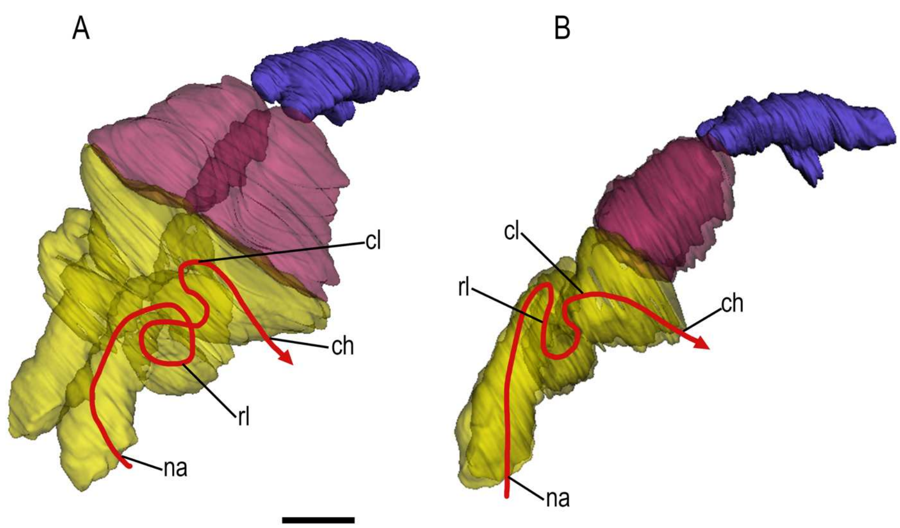

FIGURE 13. CT-based endocast of the nasal cavity in *Panoplosaurus mirus* CMN 2759. **A**, left oblique view; **B**, left lateral view. Course of the airway through the nasal cavity is indicated by the red arrow. **Abbreviations**: **ch**, choana; **cl**, caudal loop; **na**, naris; **rl**, rostral loop. Scale bar equals 5 cm.

the olfactory epithelium. As also occurs in ROM 1215, the olfactory region is mediolaterally broad at its anterior extent and gradually narrows posteriorly where it contacts the anterior-most portion of the endocast and olfactory bulbs. Witmer and Ridgley (2008) were able to discern a complex series of scroll-like laminae within the olfactory region of ROM 1215, but these elements are not visible in CMN 2759.

DISCUSSION

Our reexamination of the holotype skull of *Pan. mirus*—greatly enhanced by CT scanning—has afforded the opportunity to address various problems relating to nodosaurid anatomy, taxonomy, physiology, and ecology. These issues are not unrelated but rather feed one into the next (e.g., variation in anatomy informs taxonomic interpretation, which in turn informs paleoecological interpretation). We thus address them in sequence below.

Variability in Cranial Shape and Proportions

For nearly a century, the North American nodosaurids *Panoplosaurus* and *Edmontonia* have been considered closely related, but how to appropriately capture that relationship taxonomically has not been clear (Bakker, 1988; Burns, 2015; Carpenter, 1990; Coombs, 1971, 1978; Gilmore, 1930). Although the recognition of two genera and three species (*Pan. mirus*, *Ed. longiceps*, and *Ed. rugosidens*) has remained stable since the revision of Carpenter (1990), the assignment of specimens to these taxa has continued to be troublesome (Arbour & Currie, 2016; Coombs & Deméré, 1996; Gangloff, 1995). Much of the uncertainty surrounding these referrals stems from overlap in cranial shape and proportions across specimens assigned to *Panoplosaurus* and *Edmontonia*, which, despite having been investigated and discussed several times, has not yielded any confidently taxonomically informative patterns (Bakker, 1988; Burns, 2015; Carpenter, 1990; Coombs, 1971; Gangloff, 1995; Stanford et al., 2011). Most recently, Stanford et al. (2011) assessed variation in cranial shape with a principal components analysis (PCA) that included *Pan. mirus* (CMN 2759, ROM 1215, TMP 1983.025.0002), *Ed. rugosidens* (USNM 11868, AMNH 5381), *Ed. longiceps* (CMN 8531, AMNH 3076, DMNH 468), *Paw. campbelli* (SMU 73203), and the purported nodosaurid hatchling *Propanoplosaurus marylandicus* (USNM 540686). They found that the size of the skull mid-region (an area equivalent to the position of the internasal caputegulum) and snout length (PC1) along with snout width (PC2) accounted for 58.2% of the total variation, but the skulls did not form any discrete clusters that would suggest that this morphology varies among species (Stanford et al., 2011). Although Stanford et al. (2011) corrected for asymmetric distortion, many of the skulls used in their analysis have undergone some degree of dorsoventral crushing that may exaggerate certain features, including skull width (Carpenter, 1990). As such, how cranial shape may or may not vary across *Panoplosaurus* and *Edmontonia* remains uncertain and, consequently, remains problematic for the referral of specimens.

Within *Panoplosaurus*, Carpenter (1990) argued that the shortened skull of CMN 2759 relative to the more elongate ones of referred specimens cannot be attributed to taphonomic distortion. He instead suggested that the shortened skull may result from the shorter snout in CMN 2759 and considered it to represent either a juvenile or a sexually dimorphic trait (Carpenter, 1990). Indeed, CMN 2759 was shown to have the shortest snout among all the specimens sampled by Stanford et al. (2011), and while their analysis also suggested this was ontogenetic, they proposed an opposite trend to that of Carpenter (1990). Stanford et al. (2011) found that the snout was long in the hatchling *Pr. marylandicus* whereas the skull mid-region was small and more anteriorly positioned relative to the other specimens. They proposed that, during growth, the skull mid-region expanded and shifted posteriorly while the snout shortened relative to the rest of the skull (Stanford et al., 2011). Interestingly, ROM 1215 corresponded closely to the cranial morphology of *Pr. marylandicus*, suggesting that it may represent a young individual. Among the referred *Panoplosaurus* specimens for which the internasal caputegulum is present, this element is smaller in ROM 1215 than in TMP 1998.067.0001 and possibly DPMWA 90-25 (difficult to be certain due to the incompleteness of this skull). The individual caputegulae are also well defined in ROM 1215 relative to other *Panoplosaurus* specimens, including CMN 2759, which was found to be a juvenile trait in the European nodosaurid *Hungarosaurus tormai* (Ősi et al., 2021). Proportional changes in the cranium during ontogeny have been documented in other dinosaur groups, including hadrosaurids (McFeeters et al., 2021; Prieto-Marquez, 2005; Wyenberg-Henzler et al., 2022), ceratopsians (Horner & Goodwin, 2006; Knapp et al., 2021; Mallon et al., 2015), sauropods (Woodruff et al., 2018), and theropods (Carr, 1999; Ratsimbaholison et al., 2016; Wang et al., 2017). Although rare, juvenile specimens of both ankylosaurids (*Eu. tutus*, *Pi. grangeri*) and nodosaurids (*Pr. marylandicus*, *H. tormai*, *Liaoningosaurus paradoxus*, 'Paw Paw scuteling') have been described and, while skeletal fusion and the development of dermal armor have been observed to coincide with growth, little is known about the ontogenetic changes in cranial shape and proportions in ankylosaurs (Burns et al., 2011; Coombs, 1986; Hill et al., 2003; Jacobs et al., 1994; Maryańska, 1971; Ősi et al., 2021; Stanford et al., 2011; Xu et al., 2001). Burns et al. (2011) did find that the snout in *Pi. grangeri* maintained the same proportions during growth, unlike the snout shortening proposed to occur in nodosaurids by Stanford et al. (2011). Ultimately, until more definitive juvenile ankylosaurs are described, any potential ontogenetic trends in cranial anatomy can only be speculated upon, and whether the findings based on *Pr. marylandicus* are indeed applicable to other nodosaurid genera remains unknown.

Cranial Ornamentation Patterns and Interspecific Variation

Variation in cranial shape and proportions can plausibly be attributed to inter- and intraspecific variation, ontogeny, or taphonomic distortion. Although individual and ontogenetic variation are observed in the cranial ornamentation of both extant and extinct species (Harvey & Gutbertlet, 2000; Mead et al., 2012; Ősi et al., 2021), distinct caputegulal patterns in *Panoplosaurus* and *Edmontonia* suggest a reliable means for distinguishing between the two genera. Differences in cranial ornamentation have been discussed by other workers, but the focus has primarily been on caputegulal texture rather than patterning, with 'lumpy' and 'smooth' caputegulae considered diagnostic of *Panoplosaurus* and *Edmontonia*, respectively (Bakker, 1988; Carpenter, 1990). The present work has shown, however, that there is a distinction in the shape, size, and number of specific caputegulae between *Panoplosaurus* and *Edmontonia*, and that these distinct patterns are consistent across referred specimens (Figs. 4, 5). In *Panoplosaurus*, the posterior border of the nares (or supranarial caputegulum, if preserved) and the nasal caputegulae are separated by a laterally extending wedge of the median narial caputegulum, whereas in both species of *Edmontonia* this wedge is absent, and the supranarial and nasal caputegulae are in direct contact. The lacrimal caputegulae in *Panoplosaurus* contact the nasal caputegulae medially, in contrast to *Edmontonia* where the medial contact is with the frontoparietal caputegulum. The lacrimal caputegulae are also smaller in *Panoplosaurus* than in *Edmontonia*, and do not extend over the dorsal surface of the skull as they do in the latter. Four to five nasal caputegulae occur in *Panoplosaurus*, whereas only two occur in *Edmontonia*. The number of postorbital caputegulae is also variable between the two genera, with the postorbital boss being covered in numerous small caputegulae in *Panoplosaurus* and two large ones in *Edmontonia*. The unique combination of these characters and the consistency of their co-occurrence within each genus strongly suggests that the distinct caputegulal patterns observed in *Panoplosaurus* and *Edmontonia* reflect taxonomic variation. This coincides with the long-held recognition that cranial ornamentation in ankylosaurs is taxonomically informative and, while intraspecific variation certainly exists, caputegulal patterns are generally conservative across various ankylosaurid taxa (Arbour et al., 2014; Arbour & Currie, 2013; Arbour & Mallon, 2017; Burns, 2008; Coombs, 1978; Ford, 2000; Wiersma & Irmis, 2018).

The unique patterns of caputegulal variation that distinguish *Panoplosaurus* from *Edmontonia* are compelling, especially as they co-occur with certain differences in cranial anatomy. For example, much of the basicranium is morphologically conservative between the two genera, but a possible source of differentiation between *Panoplosaurus* and *Ed. longiceps* was observed on the ventral surface of the basioccipital. In *Panoplosaurus*, the anterolaterally oriented basal tubera are separated by a shallow longitudinal depression, whereas in *Ed. longiceps* the basal tubera are instead separated by a longitudinal ridge. The basal tubera in *Ed. longiceps* are also oriented anteromedially rather than anterolaterally as occurs in *Panoplosaurus.* In *Ed. rugosidens*, however, both a median depression (the holotype USNM 11868) and a median ridge (referred specimen AMNH 5381) are observed, suggesting the morphology of this region may be variable across individuals of this species. As such, the potential taxonomic significance of this character, if any, would need to be assessed in additional specimens. A far more overt source of differentiation between *Panoplosaurus* and *Edmontonia* is observed in their respective vomer morphologies. The present work has confirmed the occurrence of laterally expanded vomers in CMN 2759 that close ventrally to create a hollow vomerine canal. This is similar to the condition observed in the referred *Panoplosaurus* specimen ROM 1215, except that the vomers in ROM 1215 are open ventrally, yielding the deep groove that Carpenter (1990) considered diagnostic of *Panoplosaurus*. This difference may be ontogenetic, with the enclosed vomerine canal in CMN 2759 demonstrating the mature condition while the open groove of ROM 1215 may be that of a juvenile. The vomerine canal or groove in *Panoplosaurus* is highly distinct from the keeled vomers found in both species of *Edmontonia*, which lack both a canal and ventral groove and are instead solidly formed. Further, the presence of canalled/grooved vomers only co-occur with the *Panoplosaurus* caputegulal pattern, while vomers that are solid or unmodified (i.e., lacking a ventral groove) are concurrent with only the *Edmontonia* caputegulal pattern (Table 4). This strongly supports these as taxonomically significant differences that can be reliably used for the referral of additional specimens to either *Panoplosaurus* or *Edmontonia*.

Based on these findings, the referral of the historically contentious specimen ROM 1215 to *Pan. mirus* is supported. Additionally, referral of the specimens CMN 8529, TMP 1983.025.0002, and TMP 1998.067.0001 to *Pan. mirus* is also supported. The arrangement of caputegulae in ROM 20892 (postorbital caputegulae) and the Alaskan nodosaurid DPMWA 90-25 (nasal caputegulae) suggests they are also specimens of *Pan. mirus*, but due to the highly degraded condition of these specimens, they are only tentatively referred to the species as *Panoplosaurus* cf. *Pan. mirus.*

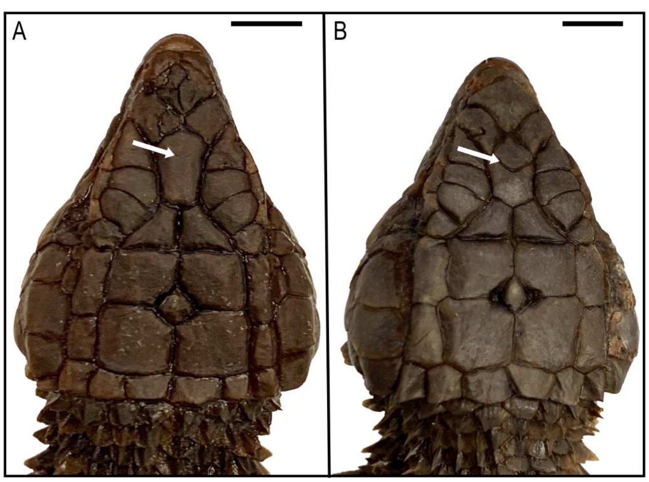

FIGURE 14. Variation in the cranial ornamentation of the extant lizard *Cordylus cordylus*. Medially located scale occurs as: **A**, a single element; **B**, a bisected element. Scale of interest is indicated by the white arrow. Scale bars equal 0.5 cm.

Caputegulal Variation within *Panoplosaurus*

The internasal caputegulum is an intriguing element that, while entirely absent in *Edmontonia*, provides a striking source of variation among specimens of *Panoplosaurus.* The internasal caputegulum is only present in some *Panoplosaurus* specimens (ROM 1215, TMP 1998.067.0001, DPMWA 90-25) while being absent in others (CMN 2759, CMN 8529, TMP 1983.025.0002). Bakker (1988) considered the presence of the internasal caputegulum, which he termed the "pre-orbital osteoderm," as a plesiomorphic trait, and this formed part of his rationale for assigning ROM 1215 to a second unnamed species of *Panoplosaurus.* Conversely, the loss of the internasal caputegulum and consequent reduction in the number of nasal caputegulae was considered a derived character and diagnostic of *Pan. mirus* (Bakker, 1988). Bakker's (1988) proposal of two species of *Panoplosaurus* has not found common acceptance, nor is it supported here. Although elements of cranial ornamentation are often highly conserved at the genus or even species level in a variety of fossil and extant vertebrates, including squamates (Harvey & Gutberlet, 2000; Montanucci, 1987; Ősi et al., 2021), crocodylians (Brazaitis, 1973; Brochu, 1999), aetosaurs (Heckert & Lucas, 1999), glyptodonts (Gillette & Ray, 1981), and armadillos (Soibelzon et al., 2013), ornamentation can also vary within a single species, resulting from ontogeny, sexual dimorphism, or individual variation (Harvey & Gutberlet, 2000; Mead et al., 2012; Ősi et al., 2021). For example, Harvey and Gutberlet (2000) found that certain species of tropidurine lizards are polymorphic in the number of circumorbital rows (scales surrounding the orbit) that occur. In the extant lizard *Cordylus cordylus*, cranial scalation patterns do not vary within a sample of 17 individuals, with a single exception: a scale situated in the midline on the snout occurs as a large single element in all individuals save one, in which this element is bisected (MCHL, pers. obs.; Fig. 14). Considering the overlap in other aspects of cranial morphology, and that Carpenter (1990) was unable to find any postcranial differences between CMN 2759 (internasal caputegulum absent) and ROM 1215 (internasal caputegulum present), variability of the internasal caputegulum may have likewise resulted from intraspecific variation within *Pan. mirus.* The variability of the internasal caputegulum is also not confined to simply being present or absent in individuals. In the referred *Panoplosaurus* specimens that have the internasal caputegulum, both the size and shape of this element varies across all three individuals (Fig. 15D–F). In those without the internasal caputegulum, there is variation in the medial furrows that divide the nasal caputegulae, forming a relatively straight line in TMP 1983.025.0002 but a sinuous one in CMN 2759 and especially CMN 8529 (Fig. 15A–C). *Panoplosaurus* specimens are also variable in their postorbital caputegulae, which appear entirely random in size, shape, and number. This suggests that both the nasal and postorbital caputegulae in *Panoplosaurus* may have been regions of considerable variability.

Buccal Osteoderms and the Implications for Cheeks

The preservation of gular and buccal osteoderms in CMN 2759 and the referred *Ed. rugosidens* specimen, AMNH 5381, suggests that these elements may have been similar in size and arrangement across both *Panoplosaurus* and *Edmontonia* (Fig. 5). The occurrence of buccal osteoderms in these specimens has also been of particular relevance to discussions of possible fleshy cheeks in ankylosaurs and other ornithischian dinosaurs. Galton (1973) proposed that muscular cheeks would have been

TABLE 4. Variation in vomer and caputegular morphology in specimens of *Panoplosaurus* and *Edmontonia*. Holotype specimens are denoted by an asterisk. **Abbreviations**: **frpaca**, frontoparietal caputegulum; **laca**, lacrimal caputegulum; **mnca**, median narial caputegulum; **nasca**, nasal caputegulum; **porb**, postorbital; **porbca**, postorbital caputegulum.

Specimen	Vomers	Number of nasca	Lateral wedge of mnca	Medial contact of laca	Number of porbca (per porb)
Panoplosaurus mirus					
CMN 2759*	canalled/grooved	4	present	nasca	>2
CMN 8529	?	4	?	?	>2
DPMWA 90-25	?	5	?	?	?
ROM 1215	canalled/grooved	5	present	nasca	>2
TMP 1983.025.0002	canalled/grooved	4	present	nasca	>2
TMP 1998.067.0001	?	5	?	?	>2
ROM 20892	?	?	?	?	>2
Edmontonia longiceps					
CMN 8531*	solid/unmodified	2	absent	frpaca	2
USNM 11868*	solid/unmodified	2	absent	frpaca	2
AMNH 5381	solid/unmodified	2	absent	frpaca	2
AMNH 5665	solid/unmodified	2	absent	frpaca	2
TMP 1991.036.0507	solid/unmodified	2	?	?	2
TMP 1998.074.0001	solid/unmodified	2	absent	?	?
UALVP 16249	solid/unmodified	2	absent	frpaca	2
Edmontonia sp.					
CMN 8879	solid/unmodified	2	?	?	?
TMP 1998.098.0001	solid/unmodified	2	absent	frpaca	2
TMP 2000.012.0158	solid/unmodified	2	absent	?	?
UALVP 55668	solid/unmodified	2	?	?	?

housed within the deeply emarginated buccal regions of ornithischians, thus preventing the loss of food during mastication. Several workers have since regarded the buccal osteoderms of *Panoplosaurus* and *Edmontonia* as the osteological correlates of cheeks, and strong evidence for the existence of some form of dermal tissue that would have covered the buccal emargination in ankylosaurs and potentially other ornithischian dinosaurs (Barrett, 2001; Knoll, 2008; Nabavizadeh, 2020, 2020; Ősi et al., 2017). Although not explicitly stated by Ford (2000), his description and illustration (fig. 5) of the buccal osteoderms in CMN 2759 appear to run counter to this interpretation and instead imply that there may have been some degree of fusion between these elements and the lower jaws. Based on CT scan data for AMNH 5381, however, Vickaryous (2006) determined that the buccal osteoderms were not fused to either the dentary or the maxilla. Likewise, there is no evidence of fusion between the buccal osteoderms and any cranial bones in the CT scan data for CMN 2759 (Fig. 6). This, together with the complete absence of buccal osteoderms preserved on the left side of the skull, lends further support for the interpretation that *Panoplosaurus* and *Edmontonia*, and perhaps other ankylosaurs, possessed fleshy cheeks that were embedded with osteoderms.

Paleoneurology of Ankylosauria

Panoplosaurus mirus is the third nodosaurid for which the brain endocast has been digitally reconstructed and described from CT scan data, and while it lacks the detail of those produced for *Paw. campbelli* (Paulina-Carabajal et al., 2016) and *S. austriacus* (Schade et al., 2022), it nonetheless provides important insights into the paleoneurology of nodosaurids. In general, the endocast of CMN 2759 exhibits the brain morphology considered typical of ankylosaurs more derived than *K. ieversi*, including short and laterally divergent olfactory bulbs and a pituitary that projects more or less ventrally (Hopson, 1979; Kuzmin et al., 2020). Strongly flexed endocasts with a ventrally convex medulla oblongata is considered the plesiomorphic condition within Ankylosauria and is currently proposed to have been retained within nodosaurids. Ankylosaurids, on the other hand, share the derived condition of a weakly flexed endocast and a ventrally flat medulla oblongata (Kuzmin et al., 2020). While ventrally convex in *S. austriacus*, the ventral surface of the medulla oblongata is medially depressed in CMN 2759 and flat in *Paw. campbelli* and cf. *Po. foxii*. As such, this character is more variable in nodosaurids than has been previously considered. Furthermore, the endocasts of both *Panoplosaurus* (CMN 2759, ROM 1215) and the referred *Ed. rugosidens* specimen AMNH 5381 are only modestly flexed relative to other nodosaurid taxa. This is because, unlike other nodosaurids, CMN 2759, ROM 1215, and AMNH 5381 lack the pronounced expansion in the cerebrum and cerebellum that increase the points of flexure between the different regions of the brain. These regions of dorsal expansion and resultant flexure are also variable across nodosaurid taxa (Fig. 16; Table 3). For instance, the cerebrum is markedly expanded in *Paw. campbelli* and cf. *Po. foxii*, resulting in relatively high degrees of cerebral flexure, but the pontine flexures in these taxa are modest and comparable to that of CMN 2759. Conversely, pronounced pontine flexures are observed in the European nodosaurids *S. transylvanicus*, *S. austriacus*, and *Hungarosaurus* sp. due to the occurrence of a hypertrophied cerebellar region (considered synapomorphic for these taxa by Ősi et al., 2014). Strong cerebral flexure is also observed in *S. transylvanicus*, but this character is unknown in *S. austriacus* and *Hungarosaurus* sp. as the anterior portion of the braincase has not been preserved in these taxa. Even so, these findings hint at further differentiation in the brain morphology of Nodosauridae, with a dorsally expanded cerebral region present in Early Cretaceous taxa (*Paw. campbelli*, cf. *Po. foxii*), a dorsally expanded cerebellar region in Late Cretaceous European taxa (*S. transylvanicus*, *S. austriacus*, *Hungarosaurus* sp.), and modest or minimal dorsal expansion in Late Cretaceous North American taxa (*Pan. mirus*, *Ed. rugosidens*). As such, a dichotomous approach to describing the shape of the endocast in ankylosaurs (highly flexed vs. weakly flexed) may be too simplistic, and variation in cerebral and pontine flexures may hold phylogenetic significance with respect to deeper evolutionary relationships within Ankylosauria.

In addition to informing on how the general morphology of the brain may differ across ankylosaurs, endocasts also provide insights into their paleobiology, including olfactory (discussed below) and auditory acuity. Unfortunately, the endosseous labyrinths are not discernible in CMN 2759, nor have they been reconstructed for the referred *Panoplosaurus* specimen ROM 1215, so the auditory capabilities of *Pan. mirus* relative to other

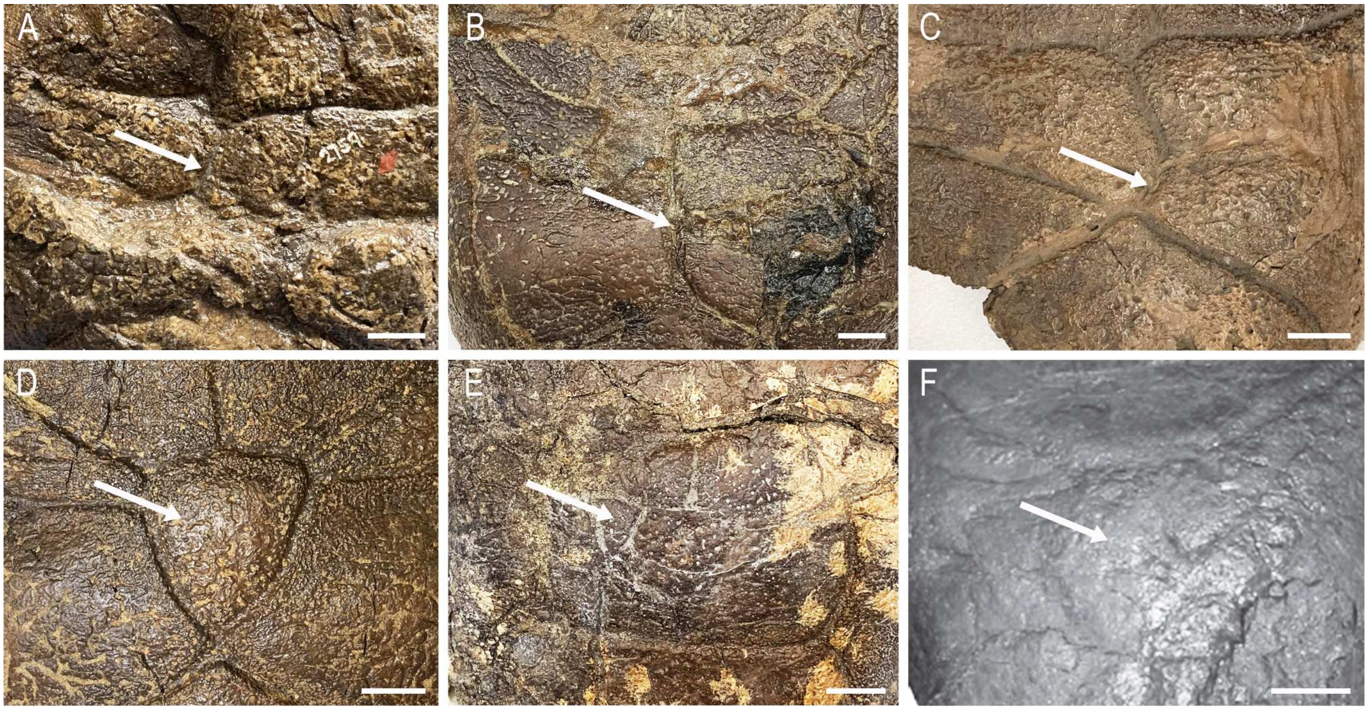

FIGURE 15. Variability in the internasal region across *Panoplosaurus* skulls in dorsal view, including variation in the furrows separating the nasal caputegulae, **A**–**C**, and variation in the size and shape of the internasal caputegulum, **D**–**F**. **A**, CMN 2759; **B**, TMP 1983.025.0002; **C**, CMN 8529; **D**, ROM 1215; **E**, TMP 1998.067.0001; **F**, DPMWA 90–25 (modified from Burns, 2015). Points of interest are indicated by the white arrow. Scale bars equal 2 cm.

ankylosaurs cannot be determined. Potential differences in the auditory capabilities of nodosaurids and ankylosaurids have been discussed elsewhere (Kuzmin et al., 2020; Paulina-Carabajal et al., 2018). The flocculus of the cerebellum is associated with the vestibulo-ocular reflex and gaze stabilization, as well as coordinated movements of the head and neck, and its presence or absence in the endocasts of ankylosaurs has been of particular interest in recent years (Buchholtz, 2012; Kuzmin et al., 2020; Paulina-Carabajal et al., 2016; Paulina-Carabajal et al., 2018; Schade et al., 2022; Walsh et al., 2013). Although the flocculus has been observed in derived ankylosaurids, it has yet to be described in the endocast of a nodosaurid, including CMN 2759, and is absent on both sides of the nearly complete endocast of AMNH 5381 (unpublished endocast provided by LMW). Based on these findings, it has been suggested that ankylosaurids required increased coordination and balance due to the active engagement of their tail clubs for defense, whereas nodosaurids were more passive in their defense strategies (Paulina-Carabajal et al., 2016; Schade et al., 2022). Increased sampling of the endocranial anatomy in ankylosaurs is needed, however, before the potential phylogenetic and paleobiological significance of the flocculus can be fully assessed.

Olfactory Capabilities

Olfaction has long been considered an important sense in ankylosaurs, and recent CT-based investigations into the endocranium of various ankylosaur taxa has supported this inference (Kuzmin et al., 2020; Maryańska, 1977; Miyashita et al., 2011; Paulina-Carabajal et al., 2016). Large olfactory regions that would have contained the sensory epithelium have been reconstructed for CMN 2759, the referred *Panoplosaurus* specimen ROM 1215, *Eu. tutus* (Witmer & Ridgley, 2008), and *Paw. campbelli* (Paulina-Carabajal et al., 2016). Large olfactory bulbs have likewise been reconstructed in various ankylosaurs, and size of the olfactory bulbs has been found to correlate positively with olfactory acuity through the increased concentration of mitral cells, odor receptors, and olfactory receptor genes (Mori et al., 1999; Steiger et al., 2008; Wenzel & Meisami, 1987; Zelenitsky et al., 2009). The olfactory ratio (greatest diameter of the olfactory bulb to the greatest diameter of the cerebral hemisphere) was proposed by Zelenitsky et al. (2009) to measure the relative olfactory capabilities in theropods, with larger values corresponding to increased olfactory acuity. This method was used by Kuzmin et al. (2020) to calculate the olfactory ratios for *K. ieversi* (58%), *Paw. campbelli* (57–63%), the referred *Panoplosaurus* specimen ROM 1215 (55–58%), *B. archibaldi* (63–69%), and *Eu. tutus* (54–59%). The olfactory ratio calculated for CMN 2759 (76%) is notably higher than those of other ankylosaurs, but the dimensions of the endocast in CMN 2759 are likely less precise than those of other ankylosaurs due to the relatively poor resolution of the CT data. In general, the high olfactory ratios indicate that olfaction was an important sense in ankylosaurs. Zelenitsky et al. (2009), however, determined that the olfactory ratios in theropods were also influenced by body size. As such, the olfactory ratios in ankylosaurs would need to be corrected for body size before olfactory acuity can be directly compared across ankylosaur taxa (Kuzmin et al., 2020; Zelenitsky et al., 2009).

Ankylosaur Nasal Passages as Thermoregulators

The nasal cavity has been digitally reconstructed from CT scan data for five ankylosaur taxa, and the results thus far reveal a morphologically complex respiratory system with remarkably elaborate nasal passages, particularly in the derived ankylosaurid *Eu. tutus* (Leahey et al., 2015; Paulina-Carabajal et al., 2016; Tumanova et al., 2025; Witmer & Ridgley, 2008). The looping morphology observed in *Eu. tutus* and the nodosaurids *Pan. mirus* and *Paw. campbelli* would have significantly increased

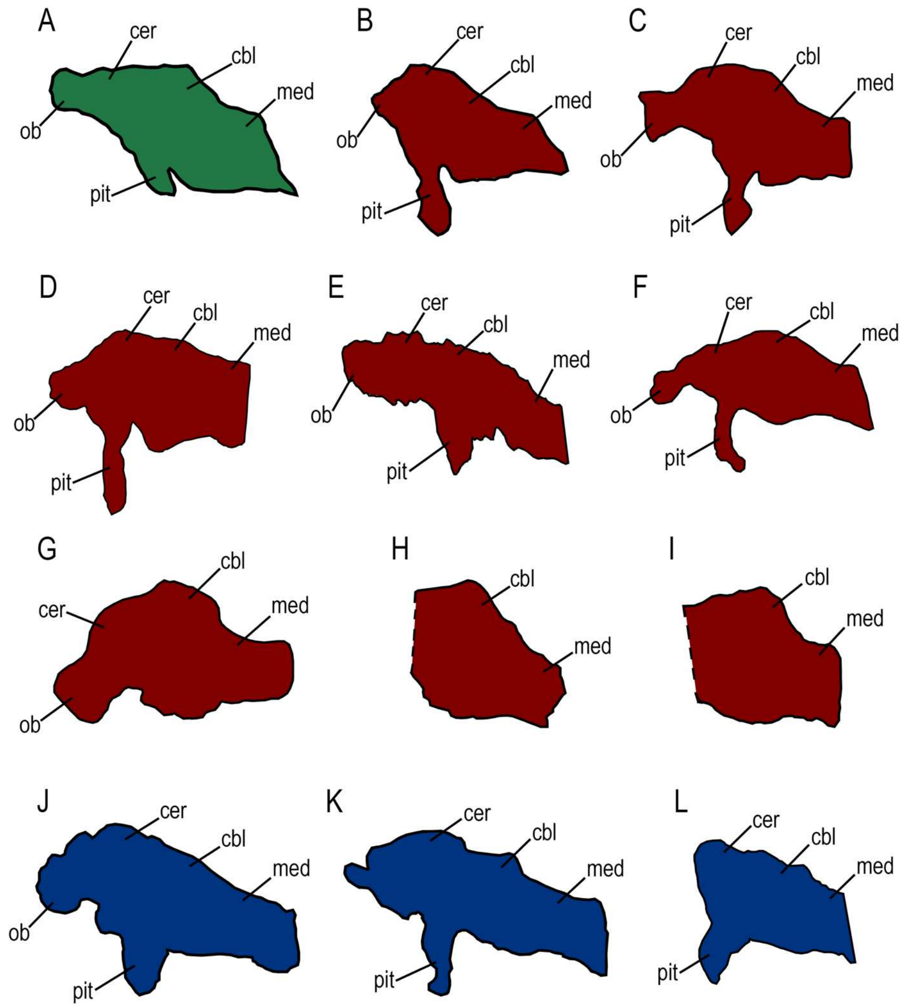

FIGURE 16. Comparison of ankylosaur brain endocasts in left lateral view. Images are color coded to represent Parankylosauria (green), Nodosauridae (red), and Ankylosauridae (blue). **A**, *Kunbarrasaurus ieversi* (modified from Leahey et al., 2015); **B**, cf. *Polacanthus foxii* (image reversed; modified from Norman & Faiers, 1996); **C**, *Pawpawsaurus campbelli* (modified from Paulina-Carabajal et al., 2016); **D**, *Edmontonia rugosidens* (AMNH 5381; modified from unpublished endocast); **E**, *Panoplosaurus mirus* (CMN 2759); **F**, *Pan. mirus* (ROM 1215; modified from Witmer & Ridgley, 2008); **G**, *Struthiosaurus transylvanicus* (modified from Ősi et al., 2014); **H**, *Struthiosaurus austriacus* (modified from Schade et al., 2022); **I**, *Hungarosaurus* sp. (modified from Ősi et al., 2014); **J**, *Euoplocephalus tutus* (modified from Miyashita et al., 2011); **K**, *Talarurus plicatospineus* (modified from Paulina-Carabajal et al., 2018), **L**, *Tarchia teresae* (modified from Paulina-Carabajal et al., 2018). **Abbreviations**: **cbl**, cerebellum; **cer**, cerebrum; **med**, medulla oblongata; **ob**, olfactory bulbs; **pit**, pituitary. Images not to scale.

the surface area of the nasal passages and inlying mucous membranes (Miyashita et al., 2011). This, coupled with evidence for extensive networks of vascularization within ankylosaur nasal cavities and braincases, has indicated that the uniquely convoluted nasal passages likely served an important function in thermoregulation (Bourke et al., 2018; Kuzmin et al., 2020; Miyashita et al., 2011; Porter & Witmer, 2020; Schade et al., 2022; Witmer & Ridgley, 2008). Bourke et al. (2018) performed a computational fluid dynamic analysis to investigate the heat exchanging efficiency in the nasal passages of *Eu. tutus* and *Pan. mirus* (ROM 1215) and found that the nasal passages in both taxa are highly efficient in warming and cooling air during inspiration and expiration, respectively. Heat exchange efficiency during exhalation resulted in estimated energy savings of 65% in *Pan. mirus* and 84% in *Eu. tutus*, with the greater efficiency in the latter being attributed to more elaborate convolutions in the nasal passages and hence, increased elongation and surface area (Bourke et al., 2018). Further, it has been suggested that the nasal passages may have cooled the venous blood circulating into the braincase of ankylosaurs, thereby maintaining thermal homeostasis of the neurosensory tissues (Bourke et al., 2018; Kuzmin et al., 2020). Insights into this system were furthered by Porter and Witmer (2020), who argued that the influx of blood being cooled in the nasal cavity before being carried in large nasal veins towards the brain and other cephalic structures was sustained by an unbalanced pattern of blood vessels (increased vasculature to the narial region and decreased vasculature to the palatal region), resulting in a regionally focused thermoregulatory strategy.

Variability of Internal Structures in *Panoplosaurus mirus*

The direct comparison of the endocranial anatomy in CMN 2759 and the referred *Panoplosaurus* specimen ROM 1215 provides the first opportunity to investigate potential intraspecific variation in the endocranium of a nodosaurid. The double looping airway that courses through the nasal cavity in CMN 2759 is indistinguishable from the one previously described for ROM 1215 (Witmer & Ridgley, 2008). These findings corroborate those from the external cranial anatomy discussed above, and the referral of ROM 1215 to *Pan. mirus* is further supported. However, it is still uncertain how the anatomy of the nasal cavity in *Pan. mirus* may have compared with that of the closely related *Edmontonia*. Two-dimensional CT slices through the cranium of the referred *Ed. rugosidens* specimen AMNH 5381 seemed to confirm the historical interpretation of simple straight nasal passages, but with the addition of a small paranasal sinus located within the maxilla (Coombs, 1978; Vickaryous, 2006). These findings were congruent with Witmer's (1997) prior interpretation of the transversely exposed nasal cavity in another *Edmontonia* specimen AMNH 3076 (considered *Edmontonia* sp. by Carpenter, 1990, and cf. *Edmontonia* here). Both specimens were reconsidered by Witmer and Ridgley (2008), and the exposed portion of the nasal cavity in AMNH 3076 was found to closely resemble the rostral loop of ROM 1215. Subsequent unpublished CT images of AMNH 5381 that were discussed by Witmer and Ridgely (2008) revealed bony laminae that could have created subdivisions within the airway. Further, Witmer and Ridgely (2008) did not find any definitive evidence of paranasal sinuses in the nasal cavity of ROM 1215, nor could we discern any in CMN 2759, and the majority of the nasal cavity in both specimens is instead occupied by the primary airway. What were initially considered a complex series of paranasal sinuses in the ankylosaurid *Eu. tutus* have also since been confirmed to be portions of the convoluted nasal passages (Coombs, 1978; Miyashita et al., 2011; Vickaryous & Russell, 2003; Witmer, 1997; Witmer & Ridgley, 2008). Taken together, these findings suggest that the nasal passages in *Edmontonia* may have been similar in complexity to those of *Pan. mirus*, but continued investigation is required.

While the morphology of the nasal passages in CMN 2759 and ROM 1215 is indistinguishable, there is observable variation in their respective brain endocasts. The cerebral and pontine flexures are similar in CMN 2759 and ROM 1215, and neither endocast is as strongly flexed as those of other nodosaurids (Table 4; Fig. 16). However, the dorsal surface of the cerebrum is higher than that of the cerebellum in CMN 2759, whereas the opposite is observed in ROM 1215 due to a more prominent dural expansion in the latter specimen. The cerebrum is more dorsoventrally expanded in CMN 2759 than ROM 1215 and displays a dorsoventral constriction just anterior to the pituitary that is absent in ROM 1215. The pituitary cavity in CMN 2759 is also more posteriorly positioned, more posteroventrally oriented, and more robust relative to ROM 1215. Although these differences may be attributed to the disparate CT scan quality between the two specimens (the resolvability of anatomical structure is considerably lower in the CT images of CMN 2759), intraspecific variation in the neural morphology of *Pan. mirus* would align with findings in other dinosaur groups (Galton, 1988; Paulina-Carabajal et al., 2021; Witmer et al., 2008). For instance, the projection of the pituitary cavity is variable in endocasts of the stegosaurid *Kentrosaurus aethiopicus* and the sauropod *Diplodocus longus*, and the relative prominence of the dural expansion in *Tyrannosaurus rex* is thought to vary at the individual level, rather than ontogenetically or taxonomically (Galton, 1988; Paulina-Carabajal et al., 2021; Witmer et al., 2008; Witmer & Ridgely, 2009). Comparison of the endocasts of CMN 2759 and ROM 1215 offer interesting insights into the potential variation in the endocranial morphology within an ankylosaur species, and further sampling among, and particularly within, other ankylosaur taxa would help elucidate these preliminary findings.

Biostratigraphic Considerations

The Dinosaur Park Formation is up to 70 m thick in the area of Dinosaur Provincial Park, Alberta (Eberth, 2005). *Panoplosaurus mirus* and *Ed. rugosidens* are, so far, the only nodosaurids known from this formation and are most abundant in (though not limited to) the lower half of the formation (Fig. 1). This pattern mirrors that of ankylosaurids in the same strata and may reflect either preservational bias or a true ecological signal (Arbour & Currie, 2013; Mallon et al., 2012).

Within their distribution, *Ed. rugosidens* appears more abundant lower in section and *Pan. mirus* higher up, with broad stratigraphic overlap of the two species between approximately 20 m and 35 m above the contact with the Oldman Formation (Fig. 1). The comparatively poor biostratigraphic sampling of *Pan. mirus* (n = 3) renders the true range of the species yet uncertain. Uncertainty about species overlap is further compounded by the fact that biostratigraphic error may range up to ± 7 m in the Dinosaur Park Formation, depending on the morphology of the ancient channel beds in which the fossils are preserved (Eberth, 2005).

Within many Upper Cretaceous strata, a single species of ankylosaurid and nodosaurid typically co-occur (Weishampel et al., 2004). In his synthetic study, Mallon (2019) attempted to account for this pattern within the Dinosaur Park Formation by showing that the co-occurring ankylosaurids and nodosaurids differ in several ecomorphological aspects, implying that their coexistence was facilitated by dietary niche partitioning (findings supported by Ballell et al., 2023 and Ősi et al., 2017). The discovery of two or more sympatric nodosaurids, which according to Mallon's (2019) model are ecomorphologically equivalent, is not predicted on the niche partitioning hypothesis; however, the hypothesis can be salvaged if (1) one of the two coexisting species is rare or (2) the temporal overlap of the two species is short-lived. Presently, both (1) and (2) appear to obtain (Fig. 1), although more data are needed. A third possibility is that *Panoplosaurus* and *Edmontonia* were ecologically distinct. If so, further investigation into the subtleties of their ecomorphology or isotopic ecology is warranted. Alternatively, food may simply not have been limiting for nodosaurids in the same way as for the remaining contemporaneous megaherbivores (ceratopsids and hadrosaurids), perhaps owing to their lower abundance on the landscape (Farlow et al., 2023; Wyenberg-Henzler et al., 2022) or to superabundance of their preferred foodstuffs. The question of megaherbivorous dinosaur coexistence continues to be ripe for exploration.

SYSTEMATIC PALEONTOLOGY

ORNITHISCHIA Seeley, 1888
THYREOPHORA Nopcsa, 1915
ANKYLOSAURIA Osborn, 1923
NODOSAURIDAE Marsh, 1890
PANOPLOSAURINI Madzia, Arbour, Boyd, Farke, Cruzado-Caballero, and Evans, 2021
PANOPLOSAURUS Lambe, 1919
PANOPLOSAURUS MIRUS Lambe, 1919

Holotype—CMN 2759, skull with articulated lower jaws, atlas, axis, cervical and dorsal vertebrae, partial synsacrum, caudal vertebrae, cervical and dorsal ribs, intersternal plate, paired xiphisternals, left scapulocoracoid, humerus, manus, tibia, fibula, pedal elements, and dermal ossifications.

Holotype Locality and Horizon—Quarry 008, Dinosaur Provincial Park, Alberta, Canada (located at 12U 463937.645E, 5620734.144N, NAD 83). The quarry occurs in the lower Dinosaur Park Formation (Megaherbivore Assemblage Zone 1 of Mallon et al., 2012), approximately 22 m above the contact with the Oldman Formation.

Amended Diagnosis (as for the Genus and Only Known Species)—Nodosaurid ankylosaur possessing the following unique combination of characters (autapomorphy identified by an asterisk), modified from Carpenter (1990): snout tapered in dorsal view; reniform ('lumpy') caputegulae; vomers laterally swollen, partially or fully enclosing hollow median canal or groove*; pterygoid foramen absent; quadrate (usually) strongly inclined with concave anterior surface; basal tubera, subtly convex longitudinal protuberances separated by shallow median depression; neural pedicels tall; neural spines tall and slender; four co-ossified sacral vertebrae; coracoid small and anteriorly rounded; scapula and coracoid co-ossified; manus tridactyl; medial cervical and anterior dorsal dermal ossifications transversely banded with paired, low-keeled plates; lateral dermal ossifications with paired high-keeled elongate plates. Further differs from *Edmontonia* in having a laterally extending wedge of the median narial caputegulum that separates the nares or supranarial caputegulae (if present) from the nasal caputegulae; four or five (if the medially positioned internasal caputegulum is present) nasal caputegulae; nasal caputegulae that contact the lacrimal caputegulae medially; and postorbital caputegulae that are numerous, small, and randomly arranged.

Referred Specimens—CMN 8529, partial cranium. ROM 1215, cranium and left lower jaw, atlas, axis, dorsal and caudal vertebrae, cervical and dorsal ribs, intersternal plate, paired xiphisternals, right scapulocoracoid, humeri, left ulna, phalanges, and dermal ossifications. TMP 1983.025.0002, cranium. TMP 1998.067.0001, cranium.

Tentatively Referred Specimens—DPMWA 90-25, partial cranium. ROM 20892 (mistakenly called ROM 1794 by Bakker, 1988), partial cranium.

Distribution—Upper Cretaceous, Dinosaur Park Formation (upper Campanian) in Alberta, Canada and (tentatively, based on DPMWA 90-25) Matanuska Formation (upper Campanian to lower Maastrichtian) in Alaska, U.S.A.

Comment—Because the present study is concerned only with the skull, the postcranial characters given by Carpenter (1990) in the amended diagnosis above remain unchanged.

EDMONTONIA Sternberg, 1928

Type Species—*Edmontonia longiceps.*

Included Species—*Edmontonia rugosidens.*

Amended Diagnosis—Nodosaurid ankylosaurs possessing the following unique combination of characters, modified from Carpenter (1990): snout parallel- or near parallel-sided in dorsal view; quadrate strongly inclined with concave anterior surface; basal tubera subtly convex longitudinal protuberances separated by shallow median depression or ridge; caputegulae smooth; neural pedicels short; neural spines short and robust; three sacral vertebrae; coracoid large and sub-squared; scapula and coracoid not co-ossified; manus tetradactyl; medial cervical and anterior dorsal dermal ossifications transversely banded with sub-rectangular and oval low-keeled plates; lateral spines. Further differs from *Pan. mirus* in that the medial borders of the lacrimal caputegulae contact the frontoparietal caputegulum; and the postorbital caputegulae are bisected.

Comment—*Edmontonia* was recovered as polyphyletic by Raven et al. (2023).

EDMONTONIA LONGICEPS Sternberg, 1928

Holotype—CMN 8531, skull with right lower jaw, dorsal vertebrae, synsacrum, caudal vertebrae, cervical and dorsal ribs, left humerus and ulna, radii, ilia, ischia, right femur and tibia, fibulae, dermal ossifications.

Holotype Locality and Horizon—11 km northwest of Morrin, Alberta, Canada on the Red Deer River, Horseshoe Canyon Formation, upper Campanian to lower Maastrichtian.

Diagnosis—Members of the genus *Edmontonia* possessing the following unique combination of characters, modified from Carpenter (1990): palate narrow; tooth rows moderately divergent; synsacrum robust: lateral spines small.

Distribution—Upper Cretaceous, Horseshoe Canyon Formation, Alberta, Canada (upper Campanian to lower Maastrichtian).

EDMONTONIA RUGOSIDENS (Gilmore, 1930) Russell, 1940

Holotype—USNM 11868, skull with right lower jaw, cervical and dorsal vertebrae, synsacrum, caudal vertebrae, ribs, ischia, right pubis, dermal ossifications.

Holotype Locality and Horizon—North side of Milk River, Blackfeet Nation, Glacier County in northern Montana, U.S.A., Two Medicine Formation, Campanian.

Diagnosis—Members of the genus *Edmontonia* possessing the following unique combination of characters, modified from Carpenter (1990): palate wide; pterygoid foramen absent; synsacrum gracile; lateral spines large.

Referred Specimens—AMNH 5381, skull with articulated lower jaws, dorsal and caudal vertebrae, ribs, left humerus, ulna, partial radius, partial manus, pelvic fragments, tibia, partial fibula, dermal ossifications. AMNH 5665, skull and anterior portion of skeleton in articulation, including cervical and dorsal vertebrae, ribs, right coracoid, scapula, and forelimb, in situ dermal ossifications. TMP 1991.036.0507, cranium. TMP 1998.074.0001, cranium. UALVP 16249, cranium.

Distribution—Upper Cretaceous, Dinosaur Park Formation (upper Campanian) in Alberta, Canada, and Two Medicine Formation (Campanian) in Montana, U.S.A.

EDMONTONIA sp.

Referred Specimens—CMN 8879, partial cranium. TMP 1998.098.0001, cranium and right lower jaw, first cervical half ring, right humerus, dermal ossifications. TMP 2000.012.0158, cranium. UALVP 55668, cranium.

Distribution—Upper Cretaceous, Dinosaur Park Formation (upper Campanian) in Alberta, Canada.

cf. *EDMONTONIA*

Referred Specimen—AMNH 3076, partial cranium.

Distribution—Upper Cretaceous, Aguja Formation in Texas, U.S.A.

CONCLUSION

The re-examination of the holotype skull of *Pan. mirus* (CMN 2759) using CT imaging has allowed the taxonomic ambiguity surrounding *Panoplosaurus* and the closely related *Edmontonia* to be addressed. The respective co-occurrence of distinct caputegulal and vomer morphologies is taxonomically significant, and the generic separation of *Panoplosaurus* and *Edmontonia* is supported. These findings provide a reliable means for differentiating between specimens of *Panoplosaurus* and *Edmontonia* and, consequently, will facilitate the appropriate generic referrals of additional specimens going forward. Further, the presence of a highly sophisticated respiratory system is confirmed, having now been described for two *Panoplosaurus* specimens, CMN 2759 and ROM 1215. Relative to other nodosaurids, the brain endocast in CMN 2759 displays less flexure, and the ventral surface of the medulla oblongata is slightly depressed rather than convex. This runs counter to the currently held understanding that the basal condition of strongly flexed endocasts with ventrally convex medullae oblongatae have been retained within Nodosauridae (Kuzmin et al., 2020; Paulina-Carabajal et al., 2018) and suggests that these characters are more variable within the clade than has thus far been considered.

It must be noted, however, that this work is limited by the quality of the CT scan data for CMN 2759; the lower resolution resulted in less detailed reconstructions of the endocranium relative to other ankylosaurs, and it is likely that the endocranial morphology that has been inferred for CMN 2759 is not as accurate as has been reported for other taxa. In addition, the external cranial anatomy of several specimens referable to *Edmontonia* was not examined first-hand for this work. The examination of relevant material is therefore less comprehensive than it could have been otherwise, and additional taxonomically significant characters may not have been captured in the present work.

As mentioned at the outset of this article, phylogenetic resolution within Nodosauridae is elusive (Arbour & Currie, 2016; Rivera-Sylva et al., 2018; Thompson et al., 2012); resolution improves with character partitioning and the culling of fragmentary taxa, but at the expense of nodosaurid monophyly (Raven et al., 2023). Thompson et al. (2012) suggested that poor phylogenetic resolution among nodosaurids may be an artifact of character construction, whereby characters fail to accurately capture variation within the clade. We highlight potential sources of variation that may be phylogenetically informative in other nodosaurids. For instance, if the systematic approach used in this work for describing cranial ornamentation is applied to nodosaurids more broadly, it could provide a valuable methodology for comparing patterns across taxa, as well as facilitating the investigation of potential phylogenetic and temporal trends in caputegulal patterns within Nodosauridae. Currently, caputegulal character states are more encompassing of ankylosaurid variability than that of nodosaurids. It is also presently unknown whether individual caputegulae are homologous across Ankylosauria, and insights may be gained through an increased investigation of nodosaurid caputegulae. Additionally, differences in both the extent of dorsal expansion and overall flexure in the brain endocasts of nodosaurids are more variable than previously considered and may be phylogenetically informative. Of course, increased sampling of the endocranium across Ankylosauria in general is needed before potential phylogenetic trends can be fully understood.

ACKNOWLEDGMENTS

We are grateful to D. Yazbek, A. Good, and the rest of the staff at the Jesse Garant Metrology Centre for CT scanning the skull of *Panoplosaurus* (CMN 2759) and providing invaluable support afterwards. We thank C. C. Mehling (AMNH), K. Seymour (ROM), and B. Strilisky (TMP) for providing collections access, and A. Ruebenstahl for generously sharing his insights into reptile palatal morphology. A special thanks to T. Dudgeon for assistance with 3D Slicer, and to A. Ayanarajan, T. Warnock-Juteau, and J. Wasserlauf for their feedback on early iterations of this manuscript. We acknowledge the Dale Patten Memorial Fund at the CMN for providing the 3D computer used for processing data from this study. This research was funded by an NSERC Discovery Grant (RGPIN-2017-06356) awarded to JCM, and by U.S. National Science Foundation grants NSF IOB-0517257, IOS-1050154, and IOS-1456503 and a Swedish Research Council grant (2021-02973) to LMW. Our research was conducted on the traditional and unceded territories of the Algonquin Anishinabeg Nation.

AUTHOR CONTRIBUTIONS

MCHL conceived and designed the project, collected and interpreted the data, and drafted the manuscript; JCM conceived and designed the project; LMW collected and interpreted the data. All authors edited the manuscript.

DATA AVAILABILITY STATEMENT

Raw data were generated at the CMN. Derived data supporting the findings of this study are available online via MorphoSource (https://doi.org/10.17602/M2/M797978).

DISCLOSURE STATEMENT

No potential conflict of interest was reported by the author(s).

ORCID

Marissa C. H. Livius http://orcid.org/0009-0004-5682-4495
Lawrence M. Witmer http://orcid.org/0000-0002-7610-0118
Michael J. Ryan http://orcid.org/0000-0001-6039-3748
Hillary C. Maddin http://orcid.org/0000-0002-6969-4907
Jordan C. Mallon http://orcid.org/0000-0002-8209-8827

LITERATURE CITED

3D Slicer (2019). *3D Slicer image computing platform* (Version 4.10.2) [Computer software]. https://www.slicer.org/

Arbour, V. M., Burns, M. E., & Sissons, R. L. (2009). A redescription of the ankylosaurid dinosaur*Dyoplosaurus acutosquameus*Parks, 1924 (Ornithischia: Ankylosauria) and a revision of the genus. *Journal of Vertebrate Paleontology*, *29*(4), 1117–1135. doi:10.1671/039.029.0405

Arbour, V. M., Burns, M. E., Sullivan, R. M., Lucas, S. G., Cantrell, A. K., Fry, J., & Suazo, T. L. (2014). A new ankylosaurid dinosaur from the Upper Cretaceous (Kirtlandian) of New Mexico with implications for ankylosaurid diversity in the Upper Cretaceous of western North America. *PLoS ONE*, *9*(9), e108804. doi:10.1371/journal.pone.0108804

Arbour, V. M., & Currie, P. J. (2013). *Euoplocephalus tutus* and the diversity of ankylosaurid dinosaurs in the Late Cretaceous of Alberta, Canada, and Montana, USA. *PLoS ONE*, *8*(5), e62421. doi:10.1371/journal.pone.0062421

Arbour, V. M., & Currie, P. J. (2016). Systematics, phylogeny, and palaeobiogeography of the ankylosaurid dinosaurs. *Journal of Systematic Palaeontology*, *14*(5), 385–444. doi:10.1080/14772019.2015.1059985

Arbour, V. M., & Mallon, J. C. (2017). Unusual cranial and postcranial anatomy in the archetypal ankylosaur*Ankylosaurus magniventris*. *Facets*, *2*, 764–794. doi:10.1139/facets-2017-0063

Bakker, R. T. (1988). Review of the Late Cretaceous nodosauroid Dinosauria: *Denversaurus schlessmani*, a new armor-plated dinosaur from the latest Cretaceous of South Dakota, the last survivor of the nodosaurians, with comments on stegosaur-nodosaur relationships. *Hunteria*, *1*(3), 1–23.

Ballell, A., Mai, B., & Benton, M. J. (2023). Divergent strategies in cranial biomechanics and feeding ecology of the ankylosaurian dinosaurs. *Scientific Reports*, *13*(1), 18242. doi:10.1038/s41598-023-45444-1

Barrett, P. M. (2001). Tooth wear and possible jaw action of *Scelidasaurus harrisonii* Owen and a review of feeding mechanisms in other thyreophoran dinosaurs. In K. Carpenter (Ed.), *The armored dinosaurs* (pp. 25–52). Indiana University Press.

Blows, W. T. (2001). Dermal armor of the polacanthine dinosaurs. In K. Carpenter (Ed.), *The armored dinosaurs* (pp. 363–385). Indiana University Press.

Bourke, J. M., Porter, W. R., & Witmer, L. M. (2018). Convoluted nasal passages function as efficient heat exchangers in ankylosaurs (Dinosauria: Ornithischia: Thyreophora). *PLoS ONE*, *13*(12), e0207381. doi:10.1371/journal.pone.0207381

Brazaitis, P. (1973). The identification of living crocodilians. *Zoologica*, *58*, 59–101.

Brochu, C. A. (1999). Phylogenetics, taxonomy, and historical biogeography of Alligatoroidea. *Journal of Vertebrate Paleontology*, *19*(sup002), 9–100. doi:10.1080/02724634.1999.10011201

Brown, C. M., Henderson, D. M., Vinther, J., Fletcher, I., Sistiaga, A., Herrara, J., & Summons, R. E. (2017). An exceptionally preserved three-dimensional armored dinosaur reveals insights into coloration and Cretaceous predator-prey dynamics. *Current Biology*, *27*(16), 2514–2521.e3. doi:10.1016/j.cub.2017.06.071

Buchholtz, E. (2012). Dinosaur paleoneurology. In M. K. Brett-Surman, T. R. Holtz Jr., & J. O. Farlow (Eds.), *The complete dinosaur* (pp. 191–208). Indiana University Press.

Burns, M. E. (2008). Taxonomic utility of ankylosaur (Dinosauria, Ornithischia) osteoderms: *Glyptodontopelta mimus* Ford, 2000: a test case. *Journal of Vertebrate Paleontology*, *28*(4), 1102–1109. doi:10.1671/0272-4634-28.4.1102

Burns, M. E. (2015). *Intraspecific variation in the armoured dinosaurs (Dinosauria: Ankylosauria)* [Unpublished doctoral dissertation]. University of Alberta.

Burns, M. E., Currie, P. J., Sissons, R. L., & Arbour, V. M. (2011). Juvenile specimens of *Pinacosaurus grangeri* Gilmore, 1933 (Ornithischia: Ankylosauria) from the Late Cretaceous of China, with comments on the specific taxonomy of *Pinacosaurus*. *Cretaceous Research*, *32*(2), 174–186. doi:10.1016/j.cretres.2010.11.007

Carpenter, K. (1990). Ankylosaur systematics: Example using *Panoplosaurus* and *Edmontonia* (Ankylosauria: Nodosauridae). In K. Carpenter, & P. J. Currie (Eds.), *Dinosaur systematics:*

Approaches and perspectives (pp. 281–298). Cambridge University Press.

Carpenter, K. (2004). Redescription of *Ankylosaurus magniventris* Brown 1908 (Ankylosauridae) from the Upper Cretaceous of the Western Interior of North America. *Canadian Journal of Earth Sciences*, *41*(8), 961–986. doi:10.1139/e04-043

Carpenter, K., & Breithaupt, B. (1986). Latest Cretaceous occurrence of nodosaurid ankylosaurs (Dinosauria, Ornithischia) in western North America and the gradual extinction of the dinosaurs. *Journal of Vertebrate Paleontology*, *6*(3), 251–257. doi:10.1080/02724634.1986.10011619

Carpenter, K., & Everhart, M. J. (2007). Skull of the ankylosaur *Niobrarasaurus coleii* (Ankylosauria: Nodosauridae) from the Smoky Hill Chalk (Coniacian) of western Kansas. *Transactions of the Kansas Academy of Science*, *110*(1 & 2), 1–9. doi:10.1660/0022-8443(2007)110[1:SOTANC]2.0.CO;2

Carpenter, K., Kirkland, J. I., Burge, D. L., & Bird, J. (1999). Ankylosaurs (Dinosauria: Ornithischia) of the Cedar Mountain Formation, Utah, and their stratigraphic distribution. In D. Gillette (Ed.), *Vertebrate paleontology in Utah* (pp. 243–251). Utah Geological Survey Miscellaneous Publication.

Carr, T. D. (1999). Craniofacial ontogeny in Tyrannosauridae (Dinosauria, Coelurosauria). *Journal of Vertebrate Paleontology*, *19*(3), 497–520. doi:10.1080/02724634.1999.10011161

Coombs, W. P., Jr. (1971). *The Ankylosauria* [Unpublished doctoral dissertation]. Columbia University.

Coombs, W. P., Jr. (1978). The families of the ornithischian dinosaur order Ankylosauria. *Palaeontology*, *21*, 143–170.

Coombs, W. P., Jr. (1986). A juvenile ankylosaur referable to the genus *Euoplocephalus* (Reptilia, Ornithischia). *Journal of Vertebrate Paleontology*, *6*(2), 162–173). doi:10.1080/02724634.1986.10011608

Coombs, W. P., Jr., & Deméré, T. A. (1996). A Late Cretaceous nodosaurid ankylosaur (Dinosauria: Ornithischia) from marine sediments of coastal California. *Journal of Paleontology*, *70*(2), 311–326. doi:10.1017/S0022336000023404

Dong, Z. (1993). An ankylosaur (ornithischian dinosaur) from the Middle Jurassic of the Junggar Basin, China. *Vertebrata PalAsiatica*, *31*, 257–266.

Eberth, D. A. (2005). The Geology. In P. J. Currie, & E. B. Koppelhus (Eds.), *Dinosaur Provincial Park: A spectacular ancient ecosystem revealed* (pp. 54–82). Indiana University Press.

Eberth, D. A., & Kamo, S. L. (2020). High-precision U–Pb CA–ID–TIMS dating and chronostratigraphy of the dinosaur-rich Horseshoe Canyon Formation (Upper Cretaceous, Campanian–Maastrichtian), Red Deer River valley, Alberta, Canada. *Canadian Journal of Earth Sciences*, *57*(10), 1220–1237. doi:10.1139/cjes-2019-0019

Farlow, J. O., Coroian, D., Currie, P. J., Foster, J. R., Mallon, J. C., & Therrien, F. (2023). "Dragons" on the landscape: Modeling the abundance of large carnivorous dinosaurs of the Upper Jurassic Morrison Formation (USA) and the Upper Cretaceous Dinosaur Park Formation (Canada). *The Anatomical Record*, *306*(7), 1669–1696. doi:10.1002/ar.25024

Fedorov, A., Beichel, R., Kalpathy-Cramer, J., Finet, J., Fillion-Robin, J.-C., Pujol, S., Bauer, C., Jennings, D., Fennessy, F. M., Sonka, M., Buatti, J., Aylward, S. R., Miller, J. V., Pieper, S., & Kikinis, S. (2012). 3D Slicer as an image computing platform for the quantitative imaging network. *Magnetic Resonance Imaging*, *30*(9), 1323–1341. doi:10.1016/j.mri.2012.05.001

Ford, T. L. (2000). A review of ankylosaur osteoderms from New Mexico and a preliminary review of ankylosaur armor. In S. G. Lucus, & A. B. Heckert (Eds.), *New Mexico Museum of Natural History and Science Bulletin: No. 17. Dinosaurs of New Mexico* (pp. 157–176).

Fowler, D. W. (2017). Revised geochronology, correlation, and dinosaur stratigraphic ranges of the Santonian–Maastrichtian (Late Cretaceous) formations of the Western Interior of North America. *PLoS ONE*, *12*(11), e0188426. doi:10.1371/journal.pone.0188426

Galton, P. M. (1973). The cheeks of ornithischian dinosaurs. *Lethaia*, *6*(1), 67–89. doi:10.1111/j.1502-3931.1973.tb00873.x

Galton, P. M. (1983). Armored dinosaurs (Ornithischia: Ankylosauria) from the Middle and Upper Jurassic of Europe. *Palaeontographica A*, *182*, 1–25.

Galton, P. M. (1988). Skull bones and endocranial casts of stegosaurian dinosaur *Kentrosaurus* Hennig, 1915 from Upper Jurassic of Tanzania, East Africa. *Geologica et Palaeontologica*, *22*, 123–143.

Gangloff, R. A. (1995). *Edmontonia* sp., *the first record of an ankylosaur from Alaska*. *Journal of Vertebrate Paleontology*, *15*(1), 195–200. doi:10.1080/02724634.1995.10011218

Gillette, D. D., & Ray, C. E. (1981). Glyptodonts of North America. *Smithsonian Contributions to Paleobiology*, *40*(40), 1–255. doi:10.5479/si.00810266.40.1

Gilmore, C. W. (1930). On dinosaurian reptiles from the Two Medicine Formation of Montana. *Proceedings of the United States National Museum*, *77*(2839), 1–39, 18 figs., 10 pls. doi:10.5479/si.00963801.77-2839.1

Harvey, M. B., & Gutberlet, R. L. Jr. (2000). A phylogenetic analysis of the tropidurine lizards (Squamata: Tropiduridae), including new characters of squamation and epidermal microstructure. *Zoological Journal of the Linnean Society*, *128*(2), 189–233. doi:10.1111/j.1096-3642.2000.tb00161.x

Heckert, A. B., & Lucas, S. G. (1999). A new aetosaur (Reptilia: Archosauria) from the Upper Triassic of Texas and the phylogeny of aetosaurs. *Journal of Vertebrate Paleontology*, *19*(1), 50–68. doi:10.1080/02724634.1999.10011122

Hill, R. V., Witmer, L. M., & Norell, M. A. (2003). A new specimen of *Pinacosaurus grangeri* (Dinosauria: Ornithischia) from the Late Cretaceous of Mongolia: Ontogeny and phylogeny of ankylosaurs. *American Museum Novitates*, *3395*(3395), 1–29. doi:10.1206/0003-0082(2003)395<0001:ANSOPG>2.0.CO;2

Hopson, J. A. (1979). Paleoneurology. In C. Gans, R. G. Northcutt, & P. Ulinski (Eds.), *Biology of the Reptilia, Vol. 9* (pp. 39–146). Academic Press.

Horner, J. R., & Goodwin, M. B. (2006). Major cranial changes during *Triceratops* ontogeny. *Proceedings of the Royal Society B: Biological Sciences*, *273*(1602), 2757–2761. doi:10.1098/rspb.2006.3643

Hu, K., King, L., Romick, C. A., Dufeau, D. L., Witmer, L. M., Stubbs, T. L., Rayfield, E. J., & Benton, M. J. (2021). Ontogenetic endocranial shape change in alligators and ostriches and implications for the development of the non-avian dinosaur endocranium. *The Anatomical Record*, *304*(8), 1759–1775. doi:10.1002/ar.24579

Jacobs, L. L., Winkler, D. A., Murray, P. A., & Maurice, J. M. (1994). A nodosaurid scuteling from the Texas shore of the Western Interior Seaway. In K. Carpenter, K. F. Hirsch, & J. R. Horner (Eds.), *Dinosaur eggs and babies* (pp. 337–346). Cambridge University Press.

Kirkland, J. I., Alcalá, L., Loewen, M. A., Espílez, E., Mampel, L., & Wiersma, J. P. (2013). The basal nodosaurid ankylosaur *Europelta carbonensis* n. gen., n. sp. from the Lower Cretaceous (Lower Albian) Escucha Formation of Northeastern Spain. *PLoS ONE*, *8*(12), e80405. doi:10.1371/journal.pone.0080405

Knapp, A., Knell, R. J., & Hone, D. W. E. (2021). Three-dimensional geometric morphometric analysis of the skull of *Protoceratops andrewsi* supports a socio-sexual signalling role for the ceratopsian frill. *Proceedings of the Royal Society B: Biological Sciences*, *288*(1944), 20202938. doi:10.1098/rspb.2020.2938

Knoll, F. (2008). Buccal soft anatomy in *Lesothosaurus* (Dinosauria: Ornithischia). *Neues Jahrbuch für Geologie und Paläontologie - Abhandlungen*, *248*(3), 355–364. doi:10.1127/0077-7749/2008/0248-0355

Kuca, N. L. (2004). *The description and comparison of* Euoplocephalus tutus *and* Edmontonia rugosidens *crania: A review of the families of the suborder Ankylosauria and ankylosaur phylogenetic systematics* [Unpublished undergraduate dissertation]. University of Alberta.

Kuzmin, I., Petrov, I., Averianov, A., Boitsova, E., Skutschas, P., & Sues, H.-D. (2020). The braincase of *Bissektipelta archibaldi* — new insights into endocranial osteology, vasculature, and paleoneurobiology of ankylosaurian dinosaurs. *Biological Communications*, *65*(2), 85–156. doi:10.21638/spbu03.2020.201

Lambe, L. M. (1919). Description of a new genus and species (*Panoplosaurus mirus*) of an armoured dinosaur from the Belly River beds of Alberta. *Transactions of the Royal Society of Canada*, *13*, 39–50.

Leahey, L. G., Molnar, R. E., Carpenter, K., Witmer, L. M., & Salisbury, S. W. (2015). Cranial osteology of the ankylosaurian dinosaur formerly known as *Minmi* sp. (Ornithischia: Thyreophora) from the Lower Cretaceous Allaru Mudstone of Richmond, Queensland, Australia. *PeerJ*, *3*, e1475. doi:10.7717/peerj.1475

Lee, Y.-N. (1996). A new nodosaurid ankylosaur (Dinosauria: Ornithischia) from the Paw Paw Formation (Late Albian) of

Texas. *Journal of Vertebrate Paleontology*, *16*(2), 232–245. doi:10.1080/02724634.1996.10011311

Leidy, J. (1856). Notice of the remains of extinct reptiles and fishes discovered by Dr. F.V. Hayden in the badlands of the Judith River. Nebraska Territory. *Academy of Natural Sciences of Philadelphia Proceedings*, *8*, 72–73.

Madzia, D., Arbour, V. M., Boyd, C. A., Farke, A. A., Cruzado-Caballero, P., & Evans, D. C. (2021). The phylogenetic nomenclature of ornithischian dinosaurs. *PeerJ*, *9*, e12362. doi:10.7717/peerj.12362

Maidment, S. C. R., Strachan, S. J., Ouarhache, D., Scheyer, T. M., Brown, E. E., Fernandez, V., Johanson, Z., Raven, T. J., & Barrett, P. M. (2021). Bizarre dermal armour suggests the first African ankylosaur. *Nature Ecology & Evolution*, *5*(12), 1576–1581. doi:10.1038/s41559-021-01553-6

Mallon, J. C. (2019). Competition structured a Late Cretaceous megaherbivorous dinosaur assemblage. *Scientific Reports*, *9*(1), 15447. doi:10.1038/s41598-019-51709-5

Mallon, J. C., Evans, D. C., Ryan, M. J., & Anderson, J. S. (2012). Megaherbivorous dinosaur turnover in the Dinosaur Park Formation (upper Campanian) of Alberta, Canada. *Palaeogeography, Palaeoclimatology, Palaeoecology*, *350-352*, 124–138. doi:10.1016/j.palaeo.2012.06.024

Mallon, J. C., Ryan, M. J., & Campbell, J. A. (2015). Skull ontogeny in *Arrhinoceratops brachyops* (Ornithischia: Ceratopsidae) and other horned dinosaurs. *Zoological Journal of the Linnean Society*, *175*(4), 910–929. doi:10.1111/zoj.12294

Marsh, O. C. (1890). Additional characters of the Ceratopsidae, with notice of new Cretaceous dinosaurs. *American Journal of Science*, *s3-39*(233), 418–426. doi:10.2475/ajs.s3-39.233.418

Maryańska, T. (1971). New data on the skull of *Pinacosaurus grangeri* (Ankylosauria). *Palaeontologia Polonica*, *25*, 45–53.

Maryańska, T. (1977). Ankylosauridae (Dinosauria) from Mongolia. *Palaeontologia Polonica*, *37*, 85–151.

Matthew, W. D. (1922). A super-dreadnaught of the animal world, the armored dinosaur *Palaeoscincus*. *Natural History*, *22*, 333–342.

McFeeters, B., Evans, D. C., & Maddin, H. C. (2021). Ontogeny and variation in the skull roof and braincase of *Maiasaura peeblesorum* from the Two Medicine Formation of Montana, U.S.A.. *Acta Palaeontologica Polonica*, *66*(3), 485–507. doi:10.4202/app.00698.2019

Mead, J. I., Schubert, B. W., Wallace, S. C., & Swift, S. L. (2012). Helodermatid lizard from the Mio-Pliocene oak-hickory forest of Tennessee, eastern USA, and a review of monstersaurian osteoderms. *Acta Palaeontologica Polonica*, *57*(1), 111–121. doi:10.4202/app.2010.0083

Miyashita, T., Arbour, V. M., Witmer, L. M., & Currie, P. J. (2011). The internal cranial morphology of an armoured dinosaur *Euoplocephalus* corroborated by x-ray computed tomographic reconstruction. *Journal of Anatomy*, *219*(6), 661–675. doi:10.1111/j.1469-7580.2011.01427.x

Montanucci, R. R. (1987). A phylogenetic study of the horned lizards, genus *Phrynosoma*, based on skeletal and external morphology. *Contributions in Science*, *390*, 1–36. doi:10.5962/p.226824

Mori, K., Nagao, H., & Yoshihara, Y. (1999). The olfactory bulb: Coding and processing of odor molecule information. *Science*, *286*(5440), 711–715. doi:10.1126/science.286.5440.711

Nabavizadeh, A. (2020). New reconstruction of cranial musculature in ornithischian dinosaurs: Implications for feeding mechanisms and buccal anatomy. *The Anatomical Record*, *303*(2), 347–362. doi:10.1002/ar.23988

Nabavizadeh, A. (2020). Cranial musculature in herbivorous dinosaurs: A survey of reconstructed anatomical diversity and feeding mechanisms. *The Anatomical Record*, *303*(4), 1104–1145. doi:10.1002/ar.24283

Nopcsa, F. (1915). Die dinosaurier der Siebenbürgischen landesteile Ungarns. *Mitteilungen aus den Jahrbuch der Königlich Ungarnischen Geologischen Reichsanstalt*, *23*, 1–24.

Norman, D. B., & Faiers, T. (1996). On the first partial skull of an ankylosaurian dinosaur from the Lower Cretaceous of the Isle of Wight, southern England. *Geological Magazine*, *133*(3), 299–310. doi:10.1017/S0016756800009031

Osborn, H.F. (1923). Two Lower Cretaceous dinosaurs from Mongolia. *American Museum Novitates*, *95*, 1–10.

Ősi, A., Magyar, J., Rosta, K., & Vickaryous, M. (2021). Cranial ornamentation in the Late Cretaceous nodosaurid ankylosaur *Hungarosaurus*. *PeerJ*, *9*, e11010. doi:10.7717/peerj.11010

Ősi, A., Pereda Suberbiola, X., & Földes, T. (2014). Partial skull and endocranial cast of the ankylosaurian dinosaur *Hungarosaurus* from the Late Cretaceous of Hungary: Implications for locomotion. *Palaeontologia Electronica*, *17*(1), 1–18. doi:10.26879/405

Ősi, A., Prondvai, E., Mallon, J., & Bodor, E. R. (2017). Diversity and convergences in the evolution of feeding adaptations in ankylosaurs (Dinosauria: Ornithischia). *Historical Biology*, *29*(4), 539–570. doi:10.1080/08912963.2016.1208194

Paulina-Carabajal, A., Currie, P. J., Dudgeon, T. W., Larsson, H. C. E., & Miyashita, T. (2021). Two braincases of *Daspletosaurus* (Theropoda: Tyrannosauridae): anatomy and comparison[1]. *Canadian Journal of Earth Sciences*, *58*(9), 885–910. doi:10.1139/cjes-2020-0185

Paulina-Carabajal, A., Lee, Y.-N., & Jacobs, L. L. (2016). Endocranial morphology of the primitive nodosaurid dinosaur *Pawpawsaurus campbelli* from the Early Cretaceous of North America. *PLoS ONE*, *11*(3), e0150845. doi:10.1371/journal.pone.0150845

Paulina-Carabajal, A., Lee, Y.-N., Kobayashi, Y., Lee, H.-J., & Currie, P. J. (2018). Neuroanatomy of the ankylosaurid dinosaurs *Tarchia teresae* and *Talarurus plicatospineus* from the Upper Cretaceous of Mongolia, with comments on endocranial variability among ankylosaurs. *Palaeogeography, Palaeoclimatology, Palaeoecology*, *494*, 135–146. doi:10.1016/j.palaeo.2017.11.030

Pereda Suberbiola, X., & Galton, P. M. (1994). A revision of the cranial features of the dinosaur *Struthiosaurus austriacus* Bunzel (Ornithischia: Ankylosauria) from the Late Cretaceous of Europe. *Neues Jahrbuch für Geologie und Paläontologie - Abhandlungen*, *191*(2), 173–200. doi:10.1127/njgpa/191/1994/173

Pereda Suberbiola, X., & Galton, P. M. (2001). Reappraisal of the nodosaurid ankylosaur *Struthiosaurus austriacus* Bunzel from the Upper Cretaceous Gosau beds of Austria. In K. Carpenter (Ed.), *The Armored Dinosaurs* (pp. 173–210). Indiana University Press.

Porter, W. R., & Witmer, L. M. (2020). Vascular patterns in the heads of dinosaurs: Evidence for blood vessels, sites of thermal exchange, and their role in physiological thermoregulatory strategies. *The Anatomical Record*, *303*(4), 1075–1103. doi:10.1002/ar.24234

Prieto-Marquez, A. (2005). New information on the cranium of *Brachylophosaurus canadensis* (Dinosauria, Hadrosauridae), with a revision of its phylogenetic position. *Journal of Vertebrate Paleontology*, *25*(1), 144–156. doi:10.1671/0272-4634(2005)025[0144:NIOTCO]2.0.CO;2

Ramezani, J., Beveridge, T. L., Rogers, R. R., Eberth, D. A., & Roberts, E. M. (2022). Calibrating the zenith of dinosaur diversity in the Campanian of the Western Interior Basin by CA-ID-TIMS U-Pb geochronology. *Scientific Reports*, *12*(1), 16026. doi:10.1038/s41598-022-19896-w

Ratsimbaholison, N. O., Felice, R. N., & O'Connor, P. M. (2016). Ontogenetic changes in the craniomandibular skeleton of the abelisaurid dinosaur *Majungasaurus crenatissimus* from the Late Cretaceous of Madagascar. *Acta Palaeontologica Polonica*, *61*(2), 281–292.

Raven, T. J., Barrett, P. M., Joyce, C. B., & Maidment, S. C. R. (2023). The phylogenetic relationships and evolutionary history of the armoured dinosaurs (Ornithischia: Thyreophora). *Journal of Systematic Palaeontology*, *21*(1), 2205433. doi:10.1080/14772019.2023.2205433

Rivera-Sylva, H. E., Frey, E., Stinnesbeck, W., Carbot-Chanona, G., Sanchez-Uribe, I. E., & Guzmán-Gutiérrez, J. R. (2018). Paleodiversity of Late Cretaceous Ankylosauria from Mexico and their phylogenetic significance. *Swiss Journal of Palaeontology*, *137*(1), 83–93. doi:10.1007/s13358-018-0153-1

Russell, L. S. (1940). *Edmontonia rugosidens* (Gilmore) an armoured dinosaur from the Belly River series of Alberta. *University of Toronto Studies Geological Series*, *43*, 3–28.

Schade, M., Stumpf, S., Kriwet, J., Kettler, C., & Pfaff, C. (2022). Neuroanatomy of the nodosaurid *Struthiosaurus austriacus* (Dinosauria: Thyreophora) supports potential ecological differentiations within Ankylosauria. *Scientific Reports*, *12*(1). doi:10.1038/s41598-021-03599-9

Schneider, C. A., Rasband, W. S., & Eliceiri, K. W. (2012). NIH image to ImageJ: 25 years of image analysis. *Nature Methods*, *9*(7), 671–675. doi:10.1038/nmeth.2089

Seeley, H. G. (1888). I. On the classification of the fossil animals commonly named Dinosauria. *Proceedings of the Royal Society of London*, *43*(258-265), 165–171. doi:10.1098/rspl.1887.0117

Soibelzon, E., Medina, M., & Abba, A. M. (2013). Late Holocene armadillos (Mammalia, Dasypodidae) of the Sierras of Córdoba, Argentina: Zooarchaeology, diagnostic characters and their paleozoological relevance. *Quaternary International*, *299*, 72–79. doi:10.1016/j.quaint.2012.09.009

Stanford, R., Weishampel, D. B., & Deleon, V. B. (2011). The first hatchling dinosaur reported from the eastern United States: *Propanoplosaurus marylandicus* (Dinosauria: Ankylosauria) from the Early Cretaceous of Maryland, U.S.A. *Journal of Paleontology*, *85*(5), 916–924. doi:10.1666/10-113.1

Steiger, S. S., Fidler, A. E., Valcu, M., & Kempenaers, B. (2008). Avian olfactory receptor gene repertoires: Evidence for a well-developed sense of smell in birds? *Proceedings of the Royal Society B: Biological Sciences*, *275*(1649), 2309–2317. doi:10.1098/rspb.2008.0607

Sternberg, C. M. (1921). A supplementary study of *Panoplosaurus mirus*. *Royal Society of Canada Transactions*, *15*, 93–102.

Sternberg, C. M. (1928). A new armored dinosaur from the Edmonton Formation of Alberta. *Transactions of the Royal Society of Canada, series 3*, *22*, 93–106.

Thompson, R. S., Parish, J. C., Maidment, S. C. R., & Barrett, P. M. (2012). Phylogeny of the ankylosaurian dinosaurs (Ornithischia: Thyreophora). *Journal of Systematic Palaeontology*, *10*(2), 301–312. doi:10.1080/14772019.2011.569091

Tumanova, T., Penkalski, P., Gallagher, W. B., Engiles, J. B., & Dodson, P. (2025). A potentially fatal cranial pathology in a specimen of *Tarchia*. *The Anatomical Record*, *308*(4), 1278–1291. doi:10.1002/ar.25205

Vickaryous, M. K. (2006). New information on the cranial anatomy of *Edmontonia rugosidens* Gilmore, a Late Cretaceous nodosaurid dinosaur from Dinosaur Provincial Park, Alberta. *Journal of Vertebrate Paleontology*, *26*(4), 1011–1013. doi:10.1671/0272-4634(2006)26[1011:NIOTCA]2.0.CO;2

Vickaryous, M. K., Maryańska, T., & Weishampel, D. B. (2004). Ankylosauria. In D. B. Weishampel, P. Dodson, & H. Osmólska (Eds.), *Dinosauria* (2nd ed, pp. 363–392). University of California Press.

Vickaryous, M. K., & Russell, A. P. (2003). A redescription of the skull of *Euoplocephalus tutus* (Archosauria: Ornithischia): A foundation for comparative and systematic studies of ankylosaurian dinosaurs. *Zoological Journal of the Linnean Society*, *137*(1), 157–186. doi:10.1046/j.1096-3642.2003.00045.x

Vickaryous, M. K., Russell, A. P., & Currie, P. J. (2001). Cranial ornamentation of ankylosaurs (Ornithischia: Thyreophora): Reappraisal of developmental hypotheses. In K. Carpenter (Ed.), *The armored dinosaurs* (pp. 318–340). Indiana University Press.

Vickaryous, M. K., & Sire, J.-Y. (2009). The integumentary skeleton of tetrapods: Origin, evolution, and development. *Journal of Anatomy*, *214*(4), 441–464. doi:10.1111/j.1469-7580.2008.01043.x

Walsh, S. A., Iwaniuk, A. N., Knoll, M. A., Bourdon, E., Barrett, P. M., Milner, A. C., Nudds, R. L., Abel, R. L., & Dello Sterpaio, P. (2013). Avian cerebellar floccular fossa size is not a proxy for flying ability in birds. *PLoS ONE*, *8*(6), e67176. doi:10.1371/journal.pone.0067176

Wang, S., Stiegler, J., Amiot, R., Wang, X., Du, G. H., Clark, J. M., & Xu, X. (2017). Extreme ontogenetic changes in a ceratosaurian theropod. *Current Biology*, *27*(1), 144–148. doi:10.1016/j.cub.2016.10.043

Watanabe, A., Gignac, P. M., Balanoff, A. M., Green, T. L., Kley, N. J., & Norell, M. A. (2019). Are endocasts good proxies for brain size and shape in archosaurs throughout ontogeny? *Journal of Anatomy*, *234*(3), 291–305. doi:10.1111/joa.12918

Weishampel, D. B., Barrett, P. M., Coria, R. A., Le Loeuff, J., Xu, X., Sahni, A., Gomani, E. M. P., & Noto, C. R. (2004). Dinosaur distribution. In D. B. Weishampel, P. Dodson, & H. Osmólska (Eds.), *Dinosauria* ((2nd ed, pp. 517–606). University of California Press.

Wenzel, B. M., & Meisami, E. (1987). Number, size, and density of mitral cells in the olfactory bulbs of the Northern Fulmar and Rock Dove. In S. Roper, & J. Atema (Eds.), *Olfaction and taste* (pp. 700–702). Annals of the New York Academy of Sciences.

Wiersma, J. P., & Irmis, R. B. (2018). A new southern Laramidian ankylosaurid, *Akainacephalus johnsoni* gen. et sp. nov., from the upper Campanian Kaiparowits Formation of southern Utah, USA. *PeerJ*, *6*, e5016. doi:10.7717/peerj.5016

Witmer, L. M. (1997). The evolution of the antorbital cavity of archosaurs: A study in soft-tissue reconstruction in the fossil record with an analysis of the function of pneumaticity. *Journal of Vertebrate Paleontology*, *17*(sup001), 1–76. doi:10.1080/02724634.1997.10011027

Witmer, L. M., & Ridgley, R. C. (2008). The paranasal air sinuses of predatory and armored dinosaurs (Archosauria: Theropoda and Ankylosauria) and their contribution to cephalic structure. *The Anatomical Record*, *291*(11), 1362–1388. doi:10.1002/ar.20794

Witmer, L. M., & Ridgley, R. C. (2009). New insights into the brain, braincase, and ear region of tyrannosaurs (Dinosauria, Theropoda), with implications for sensory organization and behavior. *The Anatomical Record*, *292*(9), 1266–1296. doi:10.1002/ar.20983

Witmer, L. M., Ridgley, R. C., Dufeau, D. L., & Semones, M. C. (2008). Using CT to peer into the past: 3D visualization of the brain and ear regions of birds, crocodiles, and nonavian dinosaurs. In H. Endo, & R. Frey (Eds.), *Anatomical imaging: towards a new morphology* (pp. 67–87). Springer.

Woodruff, D. C., Carr, T. D., Storrs, G. W., Waskow, K., Scannella, J. B., Nordén, K. K., & Wilson, J. P. (2018). The smallest diplodocid skull reveals cranial ontogeny and growth-related dietary changes in the largest dinosaurs. *Scientific Reports*, *8*(1), 14341. doi:10.1038/s41598-018-32620-x

Wynberg-Henzler, T. R., Patterson, T., & Mallon, J. C. (2022). Ontogenetic dietary shifts in North American hadrosaurids (Dinosauria: Ornithischia). *Cretaceous Research*, *135*, 105177. doi:10.1016/j.cretres.2022.105177

Xu, X., Wang, X.-L., & You, H.-L. (2001). A juvenile ankylosaur from China. *Naturwissenschaften*, *88*(7), 297–300. doi:10.1007/s001140100233

Zelenitsky, D. K., Therrien, F., & Kobayashi, Y. (2009). Olfactory acuity in theropods: Palaeobiological and evolutionary implications. *Proceedings of the Royal Society B: Biological Sciences*, *276*(1657), 667–673. doi:10.1098/rspb.2008.1075

Handling Editor: Amy Balanoff.